An Experimental Investigation and CFD Analysis into Pressure Drop for Pneumatic Conveying of Fine Powders through Closely-Coupled Bends

A Dissertation submitted
in partial fulfillment of the requirements for
the degree of

Master of Engineering

in

Thermal Engineering

by

Amit Kumar
Registration No.: 801483004

Under the Supervision of

Dr. S.S. Mallick
(Associate Professor, MED)
and
Atul Sharma
(Lecturer, MED)

MECHANICAL ENGINEERING DEPARTMENT
THAPAR UNIVERSITY, PATIALA

July, 2016

CERTIFICATE

I hereby declare that the thesis entitled "**An experimental investigation and CFD analysis into pressure drop for pneumatic conveying of fine powders through closely-coupled bends**" is an authentic record of my work carried out as requirements for the award of the degree of **Master of Engineering** in **Thermal Engineering** at **Thapar University, Patiala** under the supervision of **Dr S. S. Mallick (Associate professor) and Mr. A. Sharma (Lecturer)**, Mechanical Engineering Department, Thapar University, Patiala during July, 2014 to July, 2016. No part of the matter embodied in this report has been submitted to any other university or institute for the award of any degree.

Amit Kumar

Date: 20/06/2016

Amit Kumar

It is certified that the above statement made by the student is correct to the best of my/our knowledge and belief.

19/6/16

Dr S. S. Mallick
Mechanical Engineering Department
Thapar University, Patiala - 147004

Atul Sharma
Mechanical Engineering Department
Thapar University, Patiala - 147004

Countersigned by

Head, Mechanical Engineering Department
Thapar University, Patiala – 147004

Dean of Academic Affairs
Thapar University, Patiala - 147004

ii

Dedicated to

my parents

Acknowledgements

The experimental investigation described in this thesis has become a reality with the help of many individuals. Although it is a hard task to list each and every one of them, the author is trying to acknowledge their support for carrying out this scientific study.

Firstly I would like to express my sincere gratitude to Dr S. S. Mallick for their invaluable guidance and encouragement. I am also very thankful to Mr. Atul Sharma, Mr. Gautam Setia and Mrs. Anu Mittal for their support in my research work.

I am also grateful to Prof. P.W. Wypych, University of Wollongong, Australia, for providing me the valuable information and relevant experimental data.

All my colleagues in Thapar University are highly appreciated for their support for the research study as well as their social support, which has made my stay in Patiala enjoyable.

All India Council for Technical Education (AICTE) is also acknowledged for their financial support in the form of a scholarship to support the research work in the Thapar University.

Finally, I express my heartiest appreciation to my parents and my close friends Madhuri Dua, Karan Sharma and Rajat Bakshi for their continuous encouragement and moral support.

Amit Kumar

Abstract

Bends play a vital role in the transportation of bulk materials in the pneumatic conveying system. They provide flexibility to the conveying line, but may also result in some undesirable effects like pressure loss, product build up and blockage. This report presents results from an investigation into the modelling of closely-coupled bend pressure drop for pneumatic conveying.

In this study, six models were evaluated and compared with the experimental results. The present experimental work has been done on 53 mm I.D. × 69 m with cement material (median particle diameter: 17 μm; particle density: 2950 kg/m^3; loose-poured bulk density: 1020 kg/m^3) and 69 mm I.D. × 168 m long pipeline with fly ash material (median particle diameter: 30 μm; particle density: 2300 kg/m^3; loose-poured bulk density: 700 kg/m^3). All the six models showed under-prediction of the pressure drop. Out of six models, Chambers and Marcus (1986), Pan and Wypych (1998), Pan(1992) showed less under-prediction than Singh and Wolfe (1972), Rossetti (1983) and Das and Meloy (2002). A new model has been introduced of the same format of Pan and Wypych (1998) with some modifications which includes the effect of material properties and radius of curvature. Modelling of solid friction factor was done by using pressure drop model of Pan and Wypych (1998) and the new model. Results show that material properties significantly affect the pressure drop through closely coupled bends. The predicted pressure drop values were found to be in reasonably good agreement with experimental pressure drop.

Computational fluid dynamics (CFD) simulation has also been done on closely-coupled bends. In simulation, effects of considering single particle size and particle size distribution of the granular phase has been analysed. From results it can be concluded that, simulation with particle size distribution shows better pressure drop prediction instead using single particle size in simulation. Results also show that, by using particle size distribution % error reduces 80% to 50%.

Keywords: Pneumatic conveying; closely-couple bends; CFD.

Contents

List of Figures

APPENDIX A

List of Tables

Nomenclature

B	Bend loss factor
D	Internal diameter of pipe (m)
Fr	Froud number of flow
g	Acceleration due to gravity (m/sec^2)
L	Length of pipe (m)
m_f	Mass flow rate of air (kg/sec)
m_s	Mass flow rate of solids (kg/sec)
m*	Solid loading Ratio
K	Constant of power function
N	Number of bends
ΔP	Pressure drop through a straight horizontal pipe (Pa)
ΔP_{bo}	Pressure drop through bend (Pa)
(ΔP_z)solid	Pressure drop due to solids for an equivalent straight length of the bend (Pa)
R_B	Radius of curvature bend (m)
r	Radius of bend pipe (m)
Re	Reynolds number
V	Superficial air velocity (m/sec)
V_o	Velocity at bend outlet (m/sec)
ρ	Density of air (kg/m^3)
ρ_o	Density of air at bend outlet
ρ_f	Air/gas only friction factor
λ_{bs}	Solid friction factor at bend
λs	Solid friction factor

Subscripts

b	Bend
f	Fluid (air)
i	Inlet condition
o	Outlet condition
s	Solids
sus	Suspension
z	Straight Horizontal Pipe

Chapter 1

Introduction and Objectives

1.1 Introduction

A pneumatic conveying system is a mode of transporting bulk solids through the pipeline with the help of a transportation gas. It has wide range applications in the various industries, such as power plants, cement, food, pharmaceutical etc (Mallick and Wypych, 2009). There are some examples of successful conveying of fine powders to rocks (having size up to 70 mm). Virtually any type of bulk solids can be pneumatically conveyed, but the solids having size more than 15 mm are not suitable for pneumatic conveying (Klinzing et al., 2009).

A typical pneumatic conveying system consists of a source of compressed gas, a product feeding device, a conveying pipeline and a receiver. Positive or negative pressure can be used to convey the materials in the pipeline. To convey potentially explosive materials an inert gas such as nitrogen can be used (Mills, 2004).

Pneumatic conveying can be categorised in two flow modes: dilute phase and dense phase. In dilute phase, all the conveying particles remain suspended in the conveying air. Air velocity also remains high in this conveying mode. In dense phase conveying, most of the material remain in non-suspension mode and moves in the series of dunes on the bottom part of the pipe with a dilute phase layer of particle above the dunes (Mallick and Wypych, 2011). In dense phase, the air velocity remains less as comparative to dilute phase. Hence, a typical dense phase system can convey more amount of product per unit mass of conveying gas as compared to a similar capacity dilute phase system (Ratnayake, 2005).

Pneumatic conveying systems have a wide range of applications in different sectors due to the following advantages (Wypych, 1989).

i. Dust-free transportation of a wide variety of bulk products.
ii. Materials can be transported vertically and horizontally by the addition of a bend in the pipeline, which makes it flexible in routing.
iii. Multiple distribution and pick-up locations are possible.
iv. Less maintenance is required.

v. A secured method to convey high-valued products.
vi. These systems can be easily automated and controlled, therefore, require less manpower.

Although conveying systems have wide range of applications yet it has some disadvantages as presented below (Klinzing et al., 2009)

i. Pneumatic conveying systems need high power.
ii. System wears due to the abrasive nature of the conveyed products.
iii. Incorrect system design can result in low throughput, pipeline blockage and product degradation etc.
iv. Limited conveying range.

1.2 Aim of the Thesis

Pneumatic conveying systems require high amount of compressed gas to convey the products, which results in high amount of power requirement. Conveying material in dense phase instead of dilute phase can lower the power consumption thereby resulting in low operating cost. This can be again a problematic situation for industries because pipeline blockage usually occurs in the dense phase conveying. To rectify the blockage problem, it is mandatory to calculate the minimum conveying gas requirement/minimum transport boundary for the dense phase conveying system (Setia et al., 2015).

In pneumatic conveying system, the requirement of minimum amount of conveying gas mainly depends on the total pipeline pressure drop. It is difficult to predict the pressure drop analytically as gas-solid flow is a complex phenomenon. So many researchers have proposed empirical models to predict the pressure drop for straight (horizontal and vertical) pipeline and bends, which are valid for a certain range of products and conveying conditions (Mallick and Wypych, 2009). Models proposed by Schuchart (1968), Singh and Wolfe (1972), Rossetti (1983), Chambers and Marcus (1986), Pan (1992), Pan and Wypych (1998) have been widely used by various researchers to measure the bend pressure drop. But these models are not found suitable for closely-coupled bends (commonly found in industries due to space constrains) (Tripathi et al., 2015). In literature, less amount of work has been reported to calculate pressure drop across the closely-coupled bends, therefore, the current study is planned to model the pressure drop across the closely-coupled bends.

In these days, due to the high cost of conducting experimental tests and with fast increment in computing power, Computational Fluid Dynamics (CFD) has become powerful tool for understanding flow characteristics in gas-solids flows. CFD offers all the flow choices, pressure distribution, and solid volume fraction that help the user to grasp and design the system (Ennil et al., 2016). Therefore, in the present study, CFD technique has been used for the prediction and validation of pressure drop across closely-coupled bends.

The main objectives of the present investigation are listed below:

a) To carry out an experimental work and develop pneumatic conveying characteristics (PCC) for closely-couple bends
b) To model the solid friction factor and validation of existing and newly developed models for the pressure drop.
c) To use computational simulation to analyse and predict the pressure drop through closely-couple bends by using Ansys FLUENT 15.0.

Chapter 2

Literature Review

2.1 Introduction

A literature review was done to understand the flow characteristics of gas-solids through bends. In this chapter components of pneumatic conveying systems, conveying flow modes, material properties, types of bends and computational fluid dynamics are discussed. The models proposed by various researchers for isolated bends, have also been studied in the literature review.

2.2 Components of pneumatic conveying system

The components of pneumatic conveying are shown in Figure 2.1:

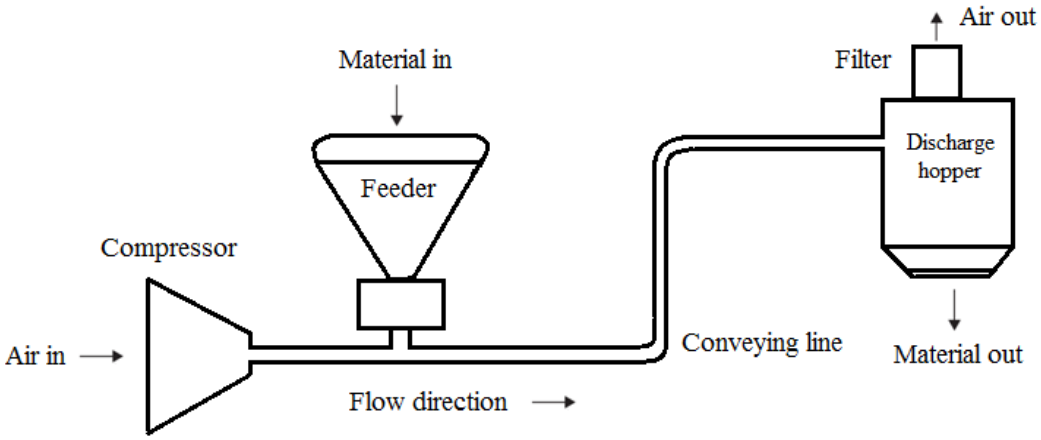

Figure 2.1 Basic components of the pneumatic conveying system

a) The prime mover

The prime mover is an essential part of the pneumatic conveying system. A wide range of compressors, blowers, fans and vacuum pumps are available to provide compressed air for pneumatic conveying. For the effective reliable working of pneumatic conveying, it is very necessary to identify the gas flow and the type of conveying (pressure or vacuum). So, according to the need of system wide range of prime movers is available for pneumatic conveying.

b) Feeding, mixing device

Feeding and mixing devices are used to mix and feed the material into the conveying line. The performance of the conveying system significantly depends on the type of the feeder. So, proper selection of these components is mandatory to satisfy the need of system requirement. Usually, blow tanks and rotary airlocks are two types of feeders which are widely used.

c) The conveying line

The conveying line is used to convey the material. The conveying line mainly consists of a network of pipelines. It includes straight pipes (horizontal and verticals) and bends. The selection of pipelines is significantly affected by a number of factors including the material properties, pipeline layout, pressure requirements etc.

d) Gas–solids separation equipments

These devices are used to separate the solids and conveying gas stream. In the pressure conveying system, some pressure drop needed across the collector to separate the solids and gas steam. The selection this system depends on a number of factors, like particle size, particle size distribution, moisture content and amount of material conveyed per unit time. In industries , different configurations of gas–solid separation systems are used like bag filters, cyclone separator, electro-static precipitator etc.

2.3 Properties of bulk solids

Material properties of the bulk materials significantly affect the behaviour of the flow in the pneumatic conveying. To characterise the materials (such as cement, fly ash, grains etc.) many descriptive terms and numerical parameters are used. The main properties of the bulk materials are listed below, which have a significant influence on the transport behaviour.

a) Particle size and distribution -- The cohesiveness of the material depends on the particle size and size distribution. As the particle size decreases the force of attraction increases which results in the increase in the cohesiveness of the material. Mean diameter, volume diameter, surface diameter etc. are some commonly known terms to define the particle size.

b) Particle shape -- particle shape is also an important characteristic as it affects the packing and flowing behaviour of the bulk materials. Highly irregular shaped or fibrous

particles can interlock results high resistance to the flow of bulk materials. Some terminologies are mentioned in the following table to characterise the shape of the bulk materials.

Table 2.1: Terminology to characterize particle shape (Kennedy and Wypych, 1990)

Term	Description
Acicular	Needle shape
Angular	Sharp edged or roughly polyhedral shape
Crystalline	Geometric shape, freely developed in fluid medium
Dendritic	Branched crystalline shape
Fibrous	Regularly or irregularly threadlike
Flaky	Plate like
Granular	Equi-diamensional, but irregular shape
Irregular	Lacking any symmetry
Nodular	Round irregular shape
Spherical	Globule shape

c) Cohesiveness -- Cohesiveness of the bulk materials is due to inter-particle attraction forces. Higher the cohesiveness of the material, high chances of the blockage in the hopper discharge, feeding and conveying as well.

d) Particle density-- As the name suggests particle density represents the actual density of a solid. Particle density shows its significant effect on transportation. It significantly affects the minimum transport velocities and air pressure requirements. The specific gravity bottle (with respect to water) method can be used to measure particle density while an air comparison pycnometer instrument can be used to determine the true volume of a known mass of particles (Wypych, 2006).

e) Bulk density-- Solid density represents the actual density of bulk solids while the bulk density of the material is a measure of the average density of the material. Bulk density not only depends on the particle density of the constituents but also the particle size (and size distribution) and shape, the packing arrangement of particles, the degree to which the particle is compacted (or aerated), the moisture content etc. Bulk density plays an important role in the design of storage vessels, feeders etc. As bulk density largely depends on the

arrangements of the particles, voids between the particles so bulk density can be change while storing or transporting the materials.

2.4 Flow modes in pneumatic conveying system

In pneumatic conveying system, for ease of classification, the flow modes are basically categorized into two distinct modes (Mallick and Wypych., 2010):

- Dilute system
- Dense system

These flow modes are categorized on the basis of suspension and non-suspension modes of conveying materials.

Dilute phase

Dilute phase sometimes referred as lean phase or suspension phase. Conveying gas stream carries the material in the suspension mode by means of lift and drag. Dilute phase is the most common method of conveying bulk materials. Most commonly products conveyed in dilute phase are flour, resins, granular and pelletized products and granular feeds etc.

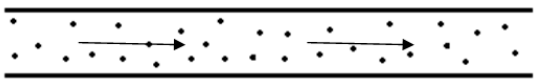

Figure 2.2: Dilute-phase pneumatic conveying

As dilute phase is widely used in industries, yet this system has some limitations.

a) In the dilute phase large amount of conveying air is used to convey the material in the suspension mode, which results higher power consumption.
b) Due to high conveying air velocity, high wear and erosion occur at the bends.

Dense phase

When the conveying gas velocity reduced to lower than the saltation velocity the particles settle down in the lower cross-section of the pipeline. In this mode only few particle remain in the suspension mode while maximum move as a series of dunes. The stable flow condition

results in smooth conveying of the material, while the unstable flow can cause sudden pressure surges as the moving layer breaks up.

Figure 2.3: Dense-phase pneumatic conveying

Types of dense phase conveying systems: There are different types of conveying modes of the dense phase conveying.

a) Fluidised dense phase
b) Low velocity slug flow
c) Low velocity plug flow
d) Single slug conveying

a) Fluidised dense phase

Fluidised dense-phase is considered a reliable and efficient method of conveying certain powders or fine granular bulk solids which can be easily fluidised and have a good air retaining property (Mainwaring et al., 1987).

Figure 2.4: Fluidised dense-phase

b) Low velocity slug flow

This mode is generally used to convey friable and/or granular products which can be deformed or crushed during the conveying. Conveying of such material is done with extremely low levels of particle damage (e.g. sugar, poly pellets, wheat and duralina) (Pan., 1992).

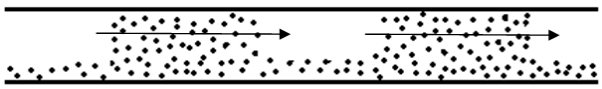

Figure 2.5: Low velocity slug flow

c) Low velocity plug flow

Low velocity plug flow transport the material as a series of discrete plugs. It also appears similar to low velocity slug flow (Wypych et al., 1990). The main difference is that low velocity plug flow does not produce a stationary layer of material. It is most recommended for cohesive or sticky powders.

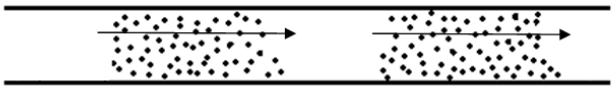

Figure 2.6: Low velocity plug flow

d) Single slug conveying

This dense-phase mode is limited to a limited batch of material per conveying cycle. A detailed description of this method of transport presented in Figure 2.7 (Wypych and Arnold, 1989).

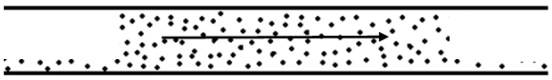

Figure 2.7: Single-slug conveying

2.5 Conveying line

The conveying line is the main component in a pneumatic conveying system. The design of conveying line is important for secure and uninterrupted conveying. Before designing pneumatic conveying line, it needs proper calculation of total pressure drop. After calculating/predicting the total pressure drop, other components of the pneumatic conveying system (i.e. compressor, dryer, air storage tank) can be choosed. Even after proper selection and installation of other components (except conveying line) blockage can occur, if designer underestimate the total pipeline pressure drop. So it needs to design of conveying line accurately.

2.6 Parts of conveying line

There are mainly two parts of conveying line:

1) Straight horizontal and vertical pipes.

2) Bends.

2.7 Types of bends

In pneumatic conveying bends play major role in system flexibility by allowing routing and distribution. There are following types of bends that are mainly used in industries as shown in fig 2.8

i. Radius bends.
ii. Blinded lateral bend.
iii. Blinded T bend.
iv. Blinded bend.
v. Mitred bend.

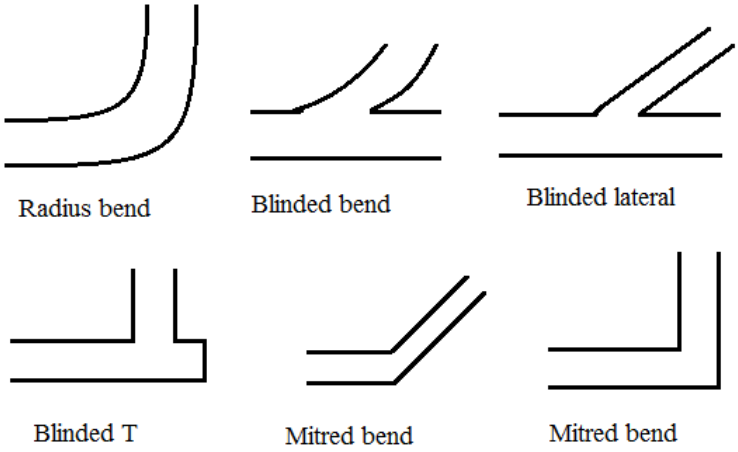

Figure 2.8: Types of bends

Selection of bends mainly depends on the conveyed material and on application. In pneumatic conveying mainly radius bends are used.

2.8 Flow through bends

When the material reaches the bend in suspension form, many factors play their role. In the single phase flows, due to change in momentum double vortex occurs at the bends and when the solid dense particles are introduced into the flow, a formation of a double vortex is further accentuated. Experimental work showed that particles also move in zig-zag motion through bends and on each impact velocity of the particles reduced (Middha et al., 2013). Due to this, particles get slow down and due to centrifugal force, they also get segregated on the outer wall of the bend, which is the formation of roping in the gas-solids flows.

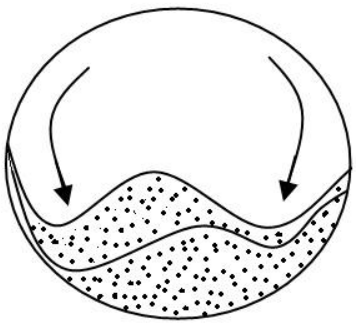

Figure 2.9: Hump profile

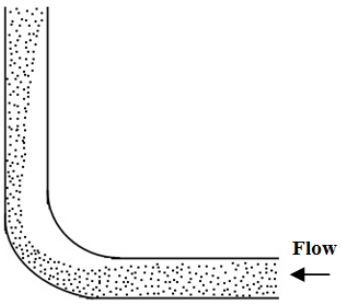

Figure 2.10: Roping formation

At the exit of the bend, due to a decrease in velocity of particles through bend a large bed deposit forms. The shape of bed downstream of the bend is also influenced by the vortex formation in the bend.

Due to this hump type profile generated in the bed as shown in Figure 2.9. This formation of the bed requires re-acceleration of the material downstream of the bend. Hence in the bends, the total pressure drop is a summation of pressure drop due to slowing down of particles in the bend and reacceleration of the particles downstream of the bend.

2.9 Pressure drop prediction through bends

For bends pressure drop prediction/calculation researchers proposed the following empirical models:

Schuchart (1968) performed experimental work on different bends (bend diameter 0.034 m and curvature radius ranging from 60-350 mm) with different materials like quartz glass (ρ_s = 2600 kg/m^3, and particle diameter d_p ranging from 1500-3000 μm) and polyamide plastic (ρ_s = 1140 kg/m^3 and particle diameter d_p = 2180 μm) with volumetric concentration up to 5% for pressure drop due to solids. From experimental results, he suggested model (Equation 2.3) for pressure drop due to solids

$$\frac{\Delta p_{bs}}{\Delta p_{zs}} = 210\left(\frac{2R_B}{D}\right)^{-1.15} \tag{2.3}$$

As mentioned in Equation 2.1 that total pressure drop is equal to the sum of both the pressure drop due to air and solids, so Equation 2.4 proposed by Ito (Ito, H., 1960) can be used to calculate pressure drop due to air only

$$\Delta p_{bf} = \left(\frac{0.029+0.304\ [Re(r/R_B)^2\ ]^{-0.25}}{(R_B/r)^{1/2}}\right)\frac{L\rho_o {V_o}^2}{2D} \tag{2.4}$$

Chambers and Marcus (1986) proposed a model for the total pressure drop through the bend. In this model author does not consider the material properties but account the outlet conditions of the pipe.

$$\Delta p_{bo} = \mathrm{NB}(1+m^*)\frac{\rho V_o^2}{2} \tag{2.5}$$

Where N is number of bends and B is the coefficient for bend loss. For this model theoretical derivation was not provided by Chambers and Marcus. Prediction error increases with increase in pipeline length greater than 500 m. However many researchers used this model for bend pressure drop prediction. Mallick (2009) used bend loss coefficient value as 0.5 (accounting the bend radius). Other researchers like Jones and Williams (2003) and Williams and Jones (2004) also used this equation to derive solid friction factor for straight pipeline by using the back calculation method.

Pan (1992) performed experiments by using different types of bends (one blind tee and four radius bends having different radii) with fly ash (ρ_p = 2197 kg/m^3, ρ_b = 634 kg/m^3,and mean particle diameter d_p =15.5 μm) and proposed a semi empirical formula by using mathematical and dimensional analysis

$$\Delta p_{bo} = m^* \lambda_s \frac{\rho_o V_o^2}{2} \quad (2.6)$$

$$\lambda_s = Y_1 (m*)^{Y_2} (Fr_o)^{Y_3} \quad (2.7)$$

This model is validated and tested for horizontal to horizontal bends. It is possible that this model may not be valid for horizontal to vertical or vertical to horizontal bends.

Pan and Wypych (1998) performed experimental work with four samples of fly ash (particle size ranging from 3.5 to 58 μm, particle density (ρ_p) 2180 to 2540 kg/m^3 and loose-poured bulk density 634 to 955 kg/m^3). Experiments were performed by varying velocity 3 to 25 m/s, and a solid loading ratio up to 130. They proposed a model for pressure loss due to bends only

$$\Delta p_{bs} = m^* \lambda_{bs} \frac{\rho_o V_o^2}{2} \quad (2.8)$$

while deriving this model Pan and Wypych (1998) consider the conveying conditions at outlet of the bend. By assuming the outlet conditions they have also derived solid friction factor for bends.

$$\lambda_s = 0.0097 (m*)^{0.5676} (Fr_o)^{0.9647} (\rho_o)^{-0.6232} \quad (2.9)$$

Singh and Wolfe (1972) have done experimental work on three bends (of pipe diameter 150mm and radius of curvature 381, 762, 1220 mm). By using non-dimensional approach he proposed a model for bend pressure drop Equation 2.10

$$\Delta p_{bo} = a_c + a_s \frac{m_s V_o}{D^2} \left(\frac{R}{D}\right)^{a_b} \quad (2.10)$$

where a_c represents the bend loss due to air and a_s and a_b are constants values. From empirical results a_c and a_b can be taken as 0.13 and -0.18 respectively and a_s can be taken as 0.00334 and 0.00537 for 45° and 90° bend angles respectively.

Rossetti (1983) performed experimental work on different bends (ratio of bend diameter to pipe diameter ranging from 2 to 8.4) by using coarse and fine materials. On the basis of experimental results he proposed a model

$$\Delta p_{bo} = (\lambda_f + \lambda_s)\frac{\rho_o {V_o}^2}{2} \quad (2.11)$$

In this model author used ρ_o and V_o values w.r.t. outlet conditions of the bend as in bends particles loss energy due to change in momentum and particle-particle and particle-wall collision, which results in high re-acceleration energy loss (Pan1992).

Westman, Michaelidies, and Thompson (1987) proposed Equation 2.12 and Equation 2.13 for value of λ_f and λ_s. These models also consider the outlet conditions of the bend due to slowing down and energy loss due to re-acceleration of particle.

$$\lambda_f = 0.167\left[1 + 17.062\left(\frac{2R_B}{D}\right)^{-1.219}\right] Re^{-0.17}\left(\frac{2R_B}{D}\right)^{0.84} \quad (2.12)$$

$$\lambda_s = \frac{5.4{m^*}^{1.293}}{Fr_o^{0.84}\left(\frac{2R_B}{D}\right)^{0.39}} \quad (2.13)$$

Das and Meloy (2002) studied the effects of closely-coupled bends on pressure drop and compared results of pressure drop of double bends, closely coupled bends and isolated bends. Author refers the conveying model suggested by Pan and Wypych (1992).

$$\Delta p_{bs} = k.\ SLR^a.\ V^b.\rho^c \quad (2.14)$$

Author modified this model by taking constant value near to zero and suggests that variation of density does not have significant contribution in pressure drop and suggest the following model for experimental calculation

$$\frac{\Delta p_{bs}}{SLR} = Y1.V^{Y2}$$

Experimental results showed that pressure drop through closely coupled bends is more than isolated bend but less that pressure drop through double bends (two single bends). Which showed that pressure drop through closely coupled bends is not equal to cumulative effect of two single bends.

2.10 Closely-coupled bends

Bends are the essential part of the conveying line as they play a vital role in system flexibility isolated bends and closely-coupled bends are used.

a) Isolated bends: When bends are spaced to enough distance that one bend has no any significant effect on flow of material through follower bend. In Figure 2.11 bend 1 and bend 2 are isolated bends. There is no influence of bend 1 on bend 2.

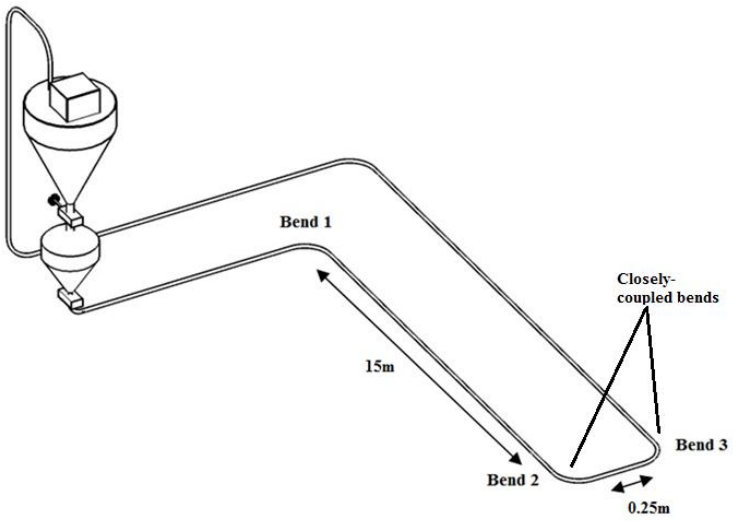

Figure 2.11: A typical layout of pipeline showing closely-coupled bends

b) Closely-coupled bends: When bends are spaced closely with not enough distance/ separation and one bend has significant effect on flow of material through follower bend. In Figure 2.11 bend 2 and bend 3 are closely-coupled bends. There is significant influence of bend 2 on bend 3.

Closely spaced bends are largely used in all powder industries due to space constraints.

2.11 Computational fluid dynamics (CFD) applications in pneumatic conveying

Use of Computational Fluid Dynamics (CFD) is increasingly in all branches of Engineering, including multi-phase applications, such as pneumatic conveying systems, slurry conveying systems etc. In this section, CFD use in pneumatic conveying is briefly described.

CFD has proven to be extremely useful and accurate for single-phase flows. Results obtained from CFD for single-phase are so accurate and precise than the results obtained from the most accurate experiments done on a physical apparatus of the same geometry. Initially, CFD applied to single phase problems, with the advances in computer processing power and more powerful numerical methods, CFD applications are now increasing in multi-phase flows. Multiphase flow involves a solid phase (or granular phases) and can be studied by using CFD. Although the behaviour of solids has never been always fully understood but attempts have been made by many researchers to simulate the multi-phase flows.

Hanley et al. (2013) presented a probabilistic analysis of particle impact at a pipe bend in pneumatic conveying. The stochastic approach has been used to quantify the breakage in particles during pneumatic conveying and assume to neglect inter-particle collision as the mean interparticle collision is lower than normal impact velocity. Du et al. (2015) carried out CFD-DEM simulation analysis formed new model to simulate the dilute phase conveying on different types of bends(horizontal-vertical, vertical-horizontal and horizontal-horizontal bends). Cui J., (2009) have done numerical modelling to predict the pressure losses caused by the different curvature radii bends. Mcglinchey et al. (2007) compared the Eulerian and mixture models to study the bend pressure drop caused by horizontal and vertically 90° bends of same curvature radii. Konan et al. (2006) compared the Euler-Euler and Euler-Lagrangian approach in horizontal channels with different wall

roughness. Kuan et al. (2003) have used Ansys Fluent to analyse the flows in single-phase and dilute phase of particulate turbulent flows through 90° duct bends (radius of curvature ranging from 1.5 to 2.0 diameter of the duct). Several turbulent models have been used for the simulation. Huang et al. (2004) have used CFD simulations to study the effects of roping formation occurred due to elbows in the pneumatic pipelines. Simulation results showed the creation and breakup mechanisms of roping. Tu et al. (1995) have used Eulerian granular approach for the simulation work on 90° square-sectioned bend.

Most of the available literature includes CFD simulation on single bends (Isolated bends) of different types (horizontal and vertical). For the closely-coupled bends, few literature is available. Das and Meloy (2002) performed only experimental work on closely-coupled bends. Also, many researchers performed simulation on gas-solid flows just by considering the mean particle diameter of the material. In actual practice, bulk materials have particle size distribution not particles of the uniform size. So the assumption of considering all the particles of the same size results a significant error in the pressure drop prediction.

This article presents a computational investigation of the influence of particle size distribution on the pressure drop through closely-coupled bends. This numerical study has been done in a steady state, incompressible and isothermal dense phase conveying of fine powder (cement) by using Ansys FLUENT 15. In this article, experimental pressure drop values are compared with the predicted pressure drop value (with and without including particle size distribution).

CHAPTER 3

Test Facility and Experimental Procedure

3.1 Introduction

Pneumatic conveying has gained a lot of popularity and has been used in many powder industries. As bends are essential components of the pipelines and causes additional pressure drop. This situation becomes more worsened when two bends are placed closely coupled. Many researchers (Schuchart (1968), Singh and wolfe (1972), Rossetti (1983), Chambers and Marcus (1986), Pan (1992), Pan and Wypych (1998) and Das and Meloy (2002)) develop empirical models for bends, but less amount of work has been reported on modelling the pressure loss of closely coupled bends. In this study evaluation of bend models and modelling the pressure loss of closely coupled has been done. Therefore it is necessary to conduct experiments.

In this chapter a brief introduction of test rigs and material properties is provided. Where necessary, a detailed description also provided of main instruments. For this thesis, test data was taken from different diameter and lengths of pipelines for the modelling of solid friction factor.

3.2 Experimental programme

For the experimental work, a new pipeline was fabricated which consists total six bends. Out of six bends, two bends are closely coupled bends. Experiments were conducted to study the behaviour of pressure drop and to model the solid friction factor for closely coupled bends. In the mean time when pipeline (Thapar University) was under fabrication, previous experimental data (University of Wollongong) was taken for the modelling purpose.

3.2.1 Properties of test products

The following material properties were considered for the purpose of evaluation of bend models and modelling of solid friction factor:

Table 3.1: Physical properties of the materials

Product	$\rho_{s\ kg/m3}$	$\rho_{b\ kg/m3}$	$d_{50\ (\mu m)}$
Fly ash	2300	700	30
White powder	1600	620	55
Cement	2950	1060	17

Particle size distribution was determined using a laser diffraction analyser (Malvern, Mastersizer 2000) and particle density was measured using a pycnometer.

3.2.2 Pneumatic conveying facilities

The following two test facilities were considered for the experimental results.

Test facility of Thapar University

For the experimental investigation, pneumatic conveying test facilities established at the Laboratory for Particle and Bulk Solids, Department of Mechanical Engineering, University of Thapar. This test rig was developed with the objective of handling the research work of both the transport modes, i.e. dilute and dense phase for wide range of gas-solid flow rates.

This test facility consists a bottom discharge blow tank of capacity 0.2 m^3 which can sustain maximum pressure 400 kPa. Experimental work was done on newly fabricated 54 mm I.D. × 69 m long pipeline on the closely-coupled bends B2 and B3. An electric powered rotary screw compressor (Model: KES 18-7.5) is used to supply air as per the test rig requirement. This compressor can supply air at maximum pressure 700 kPa with 3.37 m^3/min free air delivery. To measure the static and steady state pressure in the pipeline pressure transducers P3 and P4 were used. Location of pressure transducers is shown in Figure 1. Specification of the pressure transducers: manufacturer: Endress+Hauser ™, model: Cerabar T PMC131, pressure range: 0-4 and 0-2 bar, current signal: 4-20 mA with sample rate 500 S/s (High speed mode). Receiver bin of capacity 0.65 m^3 was installed with pulse-jet type bag filter. A refrigerated type air dryer was used to dehumidify the compressed conveying air. To avoid the intermittent supply of compressed air, an air storage tank of capacity 2 m^3 was used. Other instruments such as pressure reducing valve, non-return valve, flow meter, blow valve, pressure gauge and load cells (shear

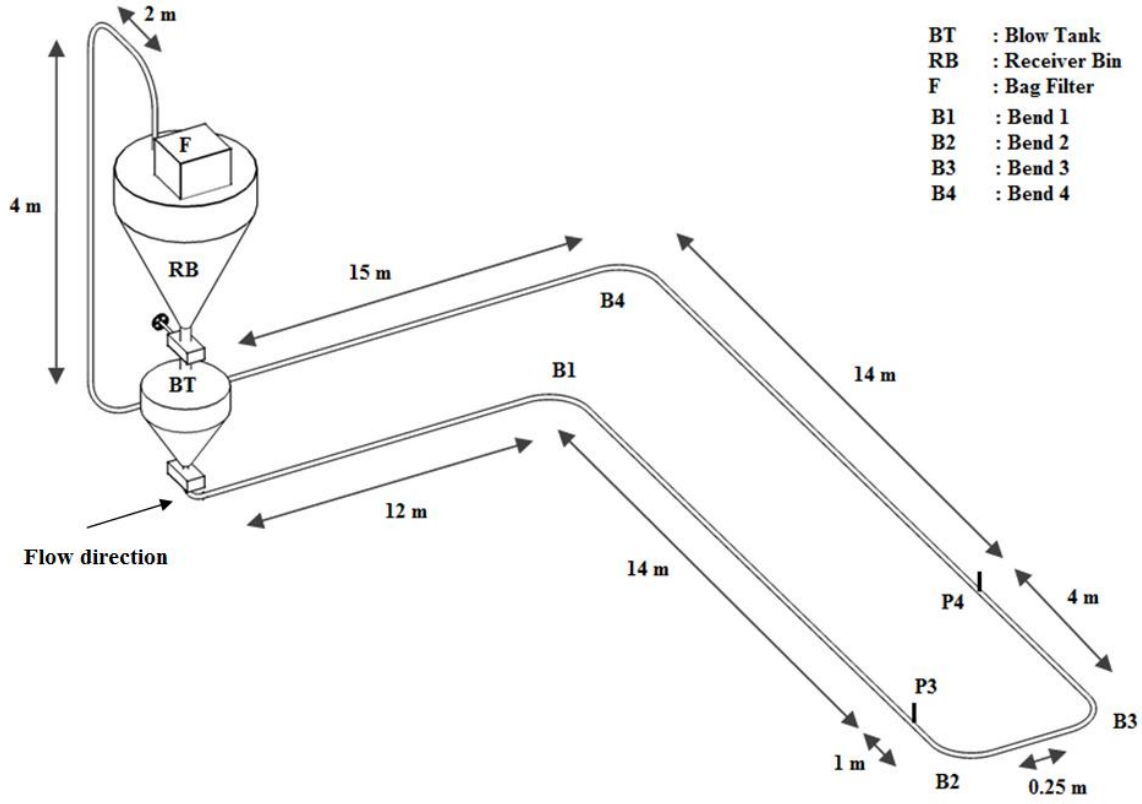

Figure 3.1: Layout of the 54 mm I.D. × 69 m long pipeline Test Rig (for Cement)

beam type) were suitably used in the layout. In the experimental work AD (analogue-digital signal conversion card) used for data acquisition NI 9208 which has a standard 37-pin D-SUB connection for use with cables and connector blocks.

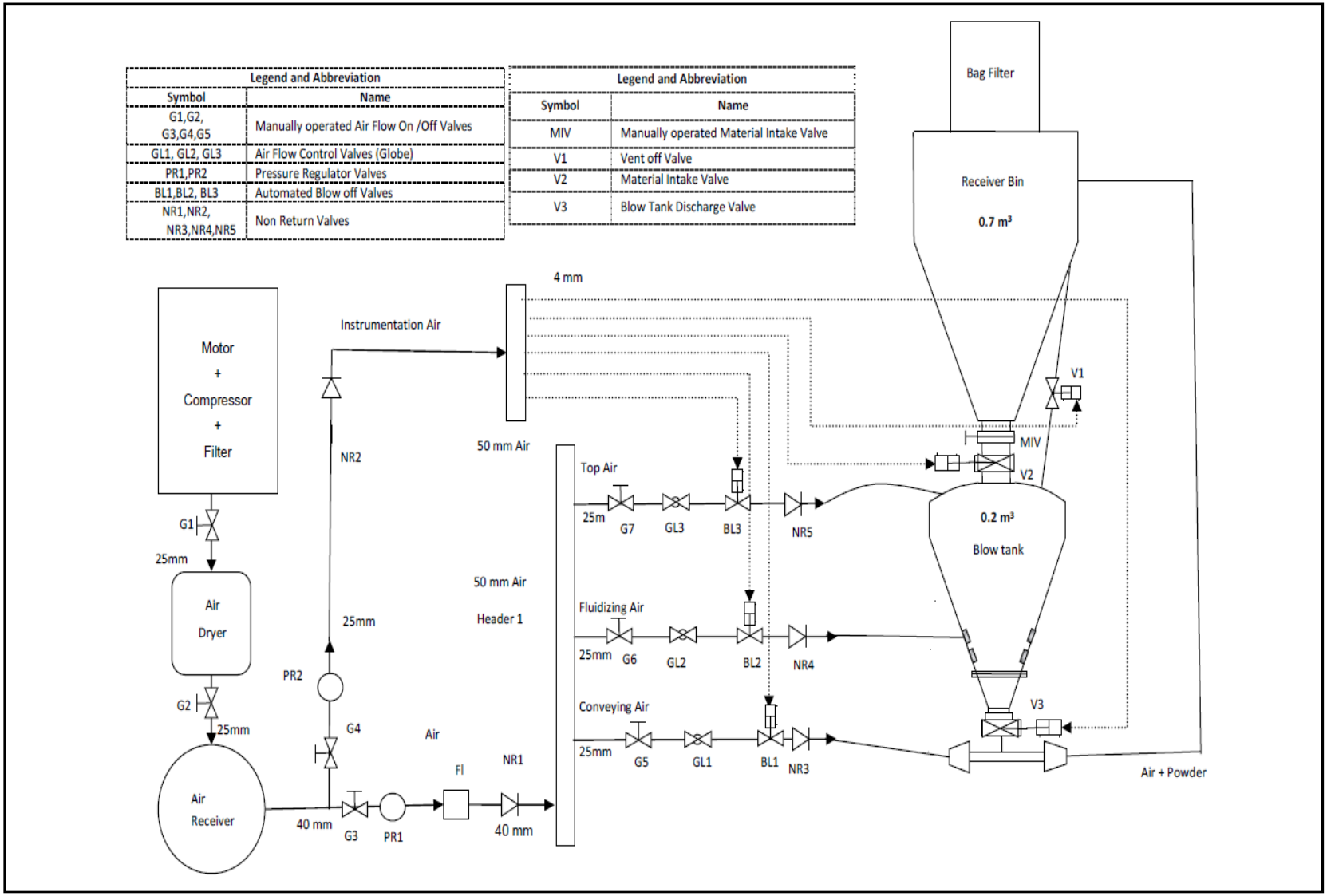

Figure 3.2: Piping and Instrumentation diagram for compressed air of 54 mm I.D. × 69m Test Rig (for cement)

Test facility of University of Wollongong

In University of Wollongong test facility used for bulk material conveying mainly consists two bottom discharge blow tanks of each 0.5 m^3 capacity. Three pipelines 69 mm I.D. × 168 m long, 105 mm I.D. × 168 m long, 69 mm I.D. × 554 m long facility is available for experimental work. Single blow tank has been used for 168m pipeline and twin blow tanks have been used for 554m pipeline. In this study modeling work was done only on 69 mm I.D. × 168 m long pipeline. Schematic diagram of 69 mm I.D. × 168 m long pipeline is as shown in Figure 3.1. 168m pipeline consists total five bends, out of which 2 bends are closely coupled bends. All bends are of 1m radius of curvature. For the leak proof connections of pipeline and bends, gaskets made up of synthetic material were used. A diesel-powered rotary screw compressor Model P375-WP was used to supply the compressed air. This compressor can supply air at maximum pressure 800 kPa with 10.6 m^3/min free air delivery. To measure the static pressure in the pipeline pressure transducers were used. Location of pressure transducers is shown in Figure 3.1. P8 is used to measure the total pipeline pressure drop.

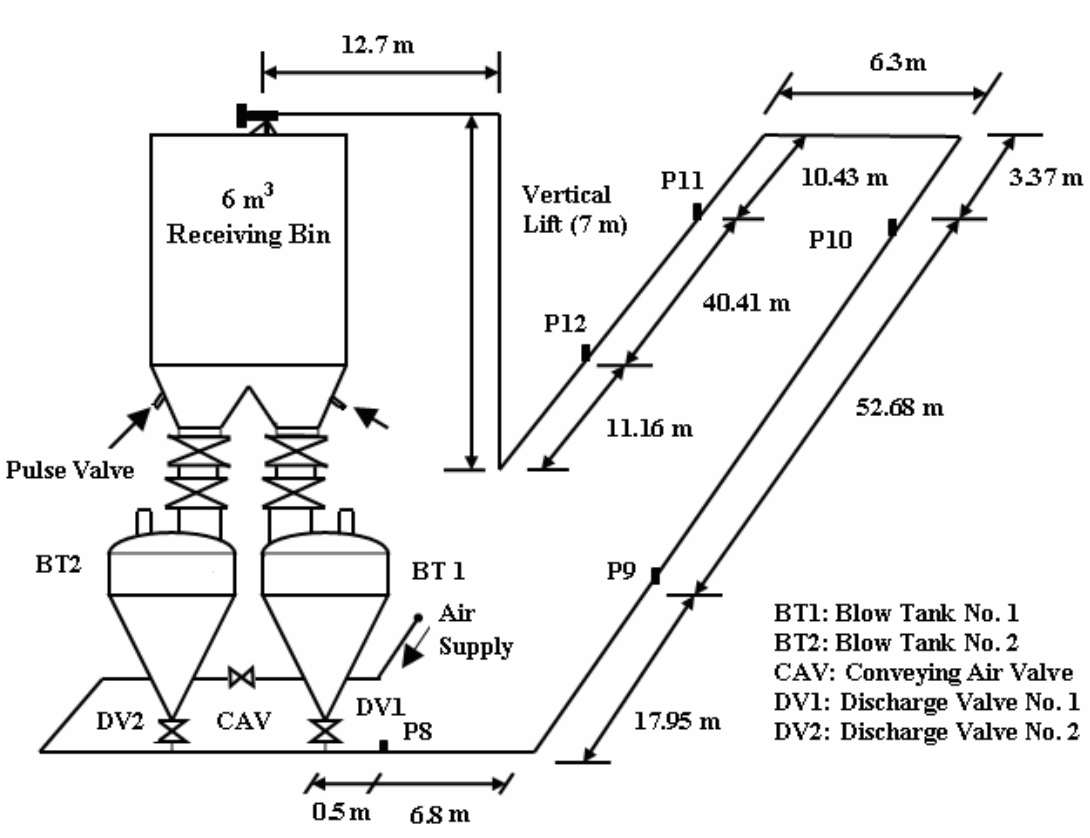

Figure 3.3: Layout of the 69 mm I.D. × 168 m long pipeline Test Rig (for fly ash)

For this study, data obtained from P10 and P11 were used to study the closely coupled bends. Specification of the pressure transducers: manufacturer: Endress and Hauser, model: Cerabar PMC133, pressure range: 0-6 and 0-2 bar, maximum pressure range: 40 bar (absolute), current signal: 4-20 mA. Receiver bin of capacity 6 m3 was installed with pulse-jet type dust filter. Other instruments such as pressure reducing valve, non-return valve, flow meter, blow valve, pressure gauge and load cells (shear beam type) were suitably used in the layout. Calibration of the transducer, load cells and flow meter was done using standardized calibration procedure. A portable data logger (Datataker 800 of Data electronics) with 24 different channels was used to record the electrical output signals from the load cells, pressure transducers and flow meter.

3.2.3 Calibrations of load cells (blow tank, receiver bin) and static pressure transducers

Load cells and pressure transducers were used to measure mass flow rate and static pressure respectively during a cycle. Load cells generate a voltage signal while pressure transducers generate a current signal. These signals must be converted to respective load and pressure units, which can only be possible by using calibration factor.

Calibration of load cells and pressure transducers was done as per the standard procedure described in Pan (1992). However, the calibration procedure of the pressure transducers is described in this section. For the calibration for transducers following steps were followed:

1) Connect all the pressure transducers by cable to the main data acquisition system.

2) With all the material in the receiver bin and after proper purging of the pipeline, close hopper valve and fill valve. Close the ball valve at the end of the pipeline, vent valve and open the discharge valve.

3) Close the blind flange upstream of the product feed point. Now increase the pressure in the line until it reaches designated pressure (e.g. 200 kPa).

4) Check for any leakage in the pipeline. If there is any leakage then open vent valve and rectify the leakage problem.

5) Now close vent valve and again start increase pressure in the pipeline in steps and note down respective current readings.

6) After getting a 5-6 reading on different pressure values, open the vent valve.

7) Now plot graphs for pressure transducers with values of current.

8) Draw a linear trend line in Excel and check display equation.

9) Values of calibration factor get display on graphs.

Table 3.2: Typical calibration results for pressure transducers.

P3	P4	Pressure (bar)
0.00595	0.00594	0.3
0.00818	0.00816	0.6
0.00966	0.00965	0.8
0.01256	0.01254	1.2
0.01416	0.01412	1.4
0.01566	0.01564	1.6
0.01685	0.01682	1.8
0.01854	0.01852	2

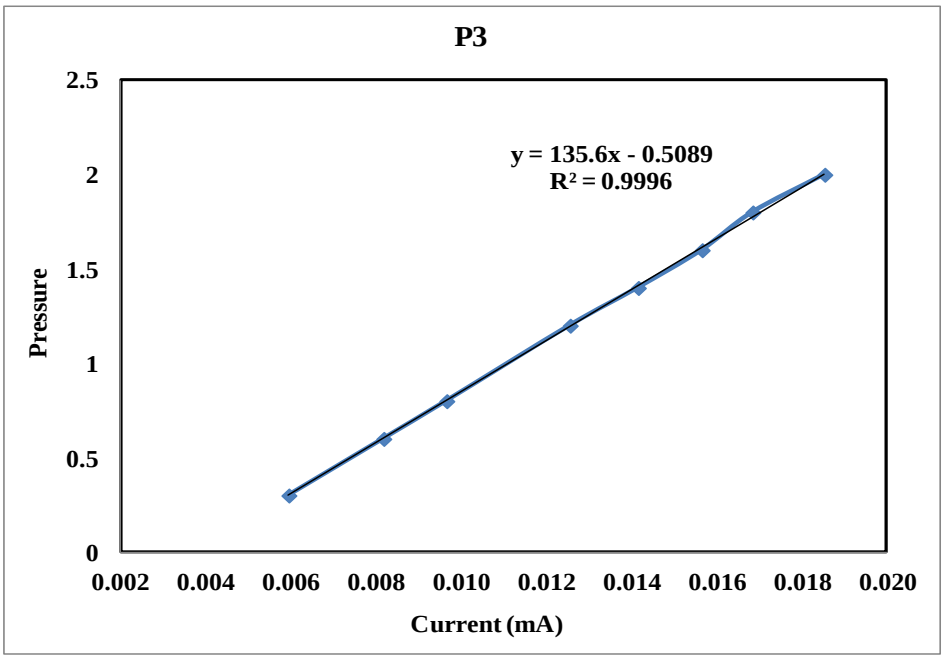

Figure 3.4: Calibration factor for P3 pressure transducer

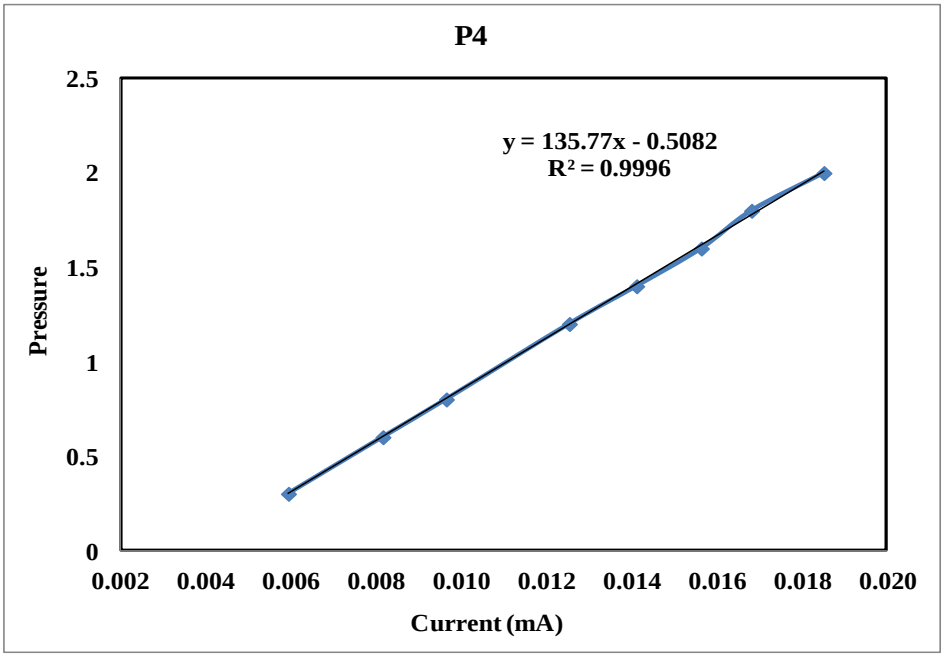

Figure 3.4: Calibration factor for P4 pressure transducer

A vortex type flow meter (40 NB diameter and of capacity up to 320 m^3/h, manufacturer: Endress+Hauser ™) was used to measure the flow rate of air in conveying cycle. This flow meter also has a digital display, which shows the reading of air volumetric flow rate. Meter also generates an analog signal which is directly sent to the data logger and reading generates in computer. To calibrate the flow meter a continual supply of air is supplied in conveying pipeline and readings of flow meter were recorded at the same time at its digital display and at data logger. Pressure data at inlet flow meter is recorded with the help of pressure transducer to make calculations for density of inlet air, in order that its mass flow rate can be obtained. The calibration of flow meter has been shown in Figure 3.6.

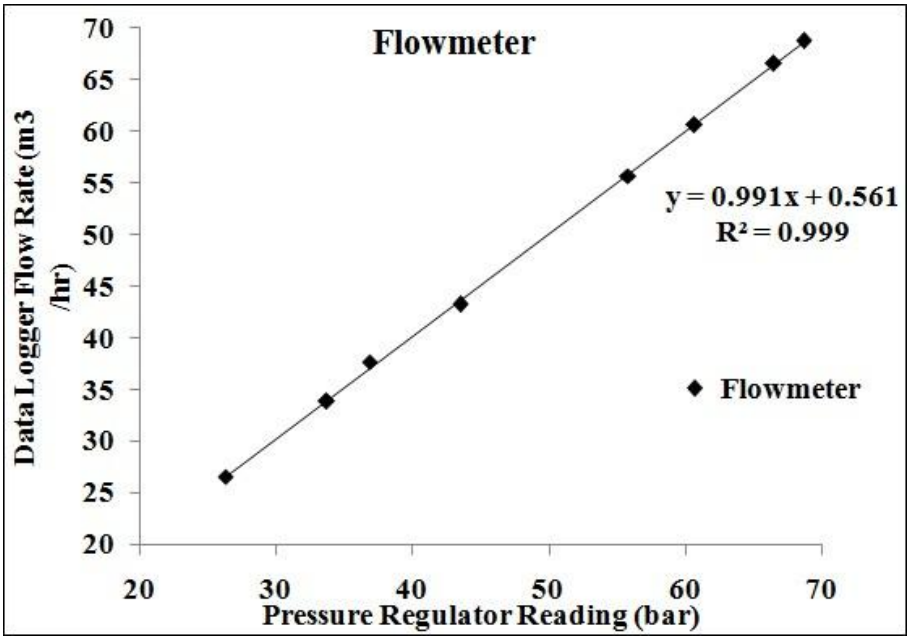

Figure 3.6: Calibration curve for flow meter

For the calculation of solid mass flow rates, both blow tank and receiver bin are supported by shear load-cells. Technical specifications are as follows:

- Manufacturing Company : HBM (Hottinger Baldwin Messtechnik)
- Model : Z6 H3
- Nominal load : 1 t
- Sensitivity (output at nominal load) : 2 mV/V
- Accuracy : ±0.1%
- Nominal range of supply voltage : 0.5-12 V

The calibration curve has been shown in Figure 3.7

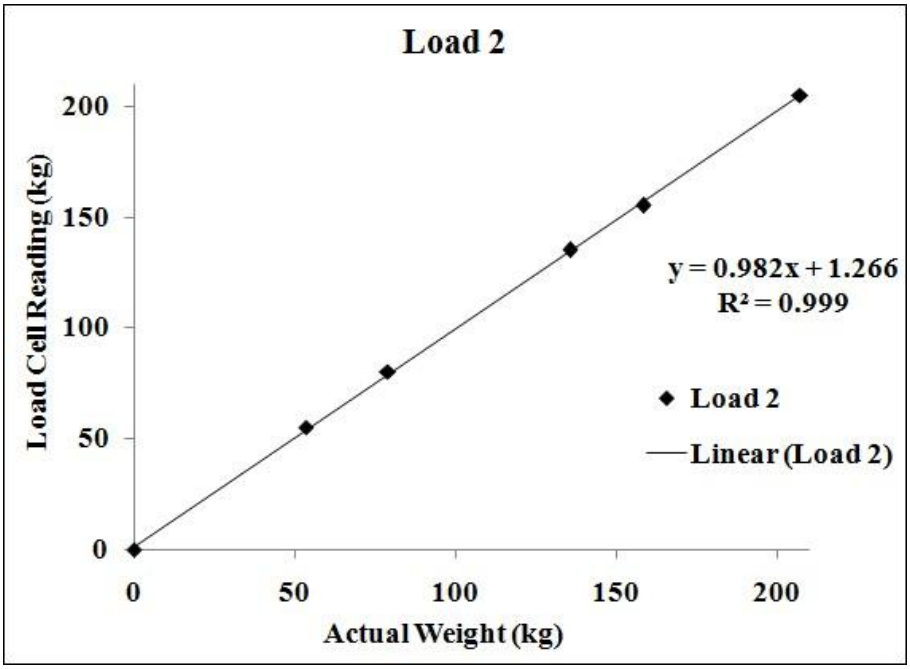

Figure 3.7: Calibration curve for load cell

3.3 Experimental procedure

In experiments, the test runs were carried out by varying the start pressure (Pressure inside blow tank) and volume flow rate of the conveying air. Wypych (1989) also suggested three approaches of the experimental procedure. To describe the experimental procedure, the whole procedure can be divided into three main sections; i.e. pre-test arrangements, testing procedure and post-test analysis (Ratnayake, C., 2005). In the pre-test arrangements setting up of the test rig, physical connections of data acquisition system, software programming of data acquisition system, etc. come under the pre-test arrangements, while post-test analysis in includes the data averaging and further relevant analysis. The explanation of general testing procedure is in the following section.

In the test rig, approximately 0.3-0.5 m^3 bulk materials were used for the experimental work. Before doing experimental work, a sample of material was tested in the laboratory for the particle size distribution. The first step in the testing procedure was filling up the receiver bin with the test material. Main supply pressure was regulated by using the pressure regulators. Generally, the preset pressure values were kept in the range of 2-4 bar. After starting the cycle, air starts to come from the main air supply and pressurises the blow tank gradually. In this stage pneumatic valves used for fluidisation of material in the blow tank.

After getting the desired value of pressure inside blow tank, conveying of material was started after opening the discharge valve. The amount of pressure inside blow tank, secondary air amount can be regulated by using manually operated globe valves. As conveying started, data acquisition programme was also started. Programme shows all readings on the computer display. To avoid any blockage and for long distance conveying, secondary air also supplied. The secondary air supply can be regulated by using globe valve.

After the end of the cycle, the amount of material collected in the receiver bin can be checked from the digital display on an LED panel. Main supply valve (Blow tank outlet) gets closed and data logging programme was also stopped. Generated data in software saved in the excel file. Sample rate can be changed the settings of the software. For the experimental work, 10 samples per seconds were recorded. After that, blow tank was getting depressurise through the ventilation connection between blow tank and receiver bin.

Chapter 4

Evaluation of Bend Models, Modeling and Validation of Solid Friction Factor

4.1 Introduction

In this chapter, all the bend models evaluated on two different closely-coupled bend data.

4.2 Evaluation of bend models based on Thapar University data

Experimental work was done on 54 mm I.D. × 69 m test rig with conveying of cement material. Material properties are shown in table 3.1. In this study pressure drop was estimated by using different bend models available in the literature. The results of predicted pressure drop have been compared with the experimental pressure drop values. Results are shown in Figure 4.1. In Figure 4.1, the "dashed" line shows the experimental pressure drop while other lines show the predicted pressure drop by different bend models. This evaluation of bend models was done just to compare models and to find an appropriate model for modelling purpose.

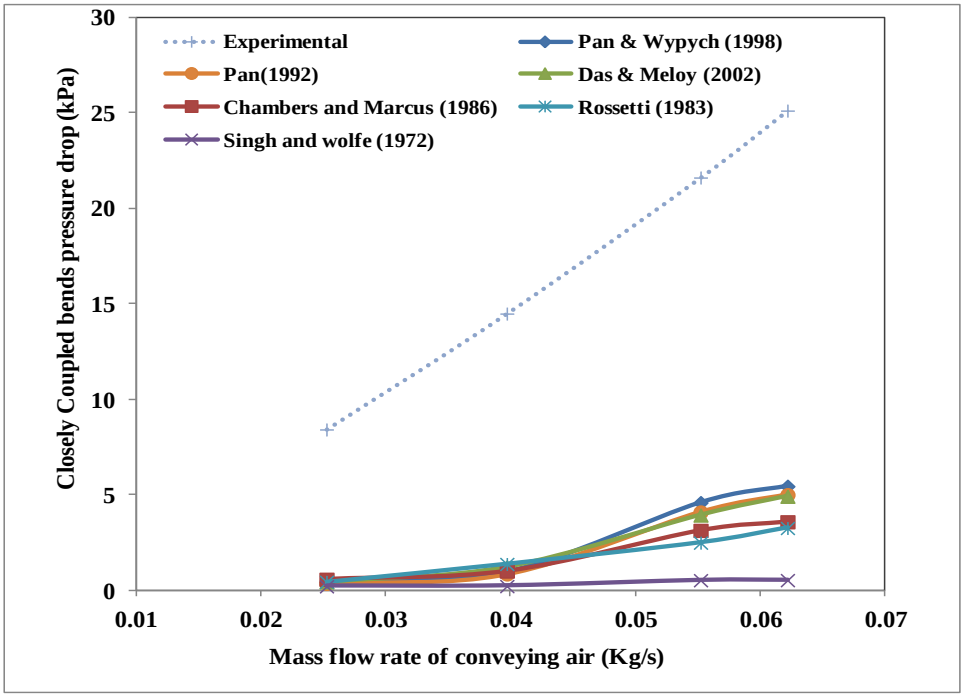

Figure 4.1: Comparison of predicted and experimental pressure drop values

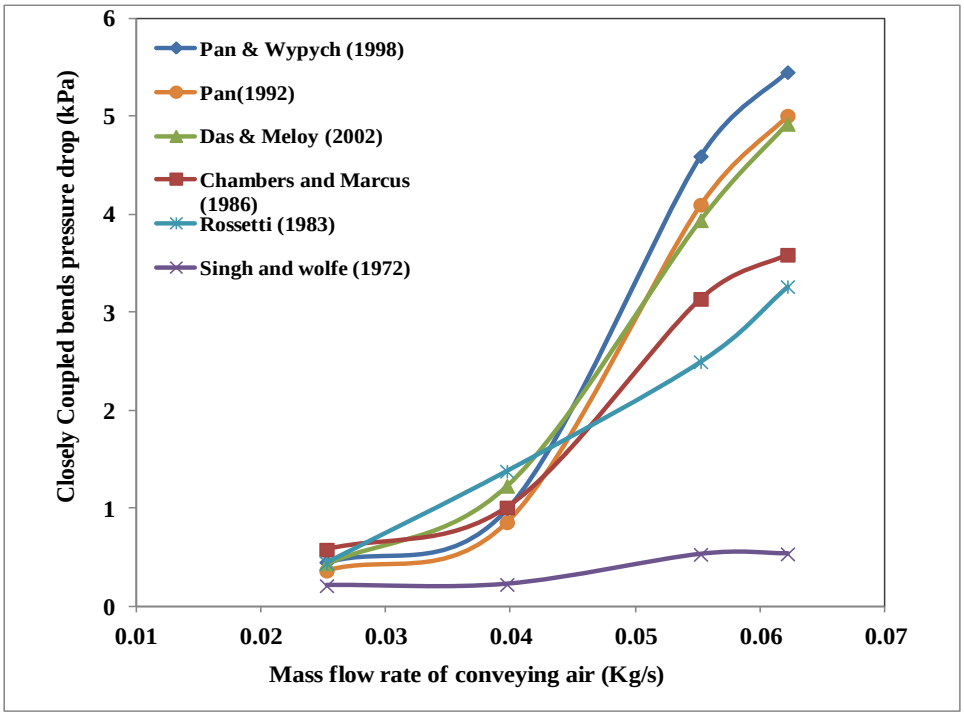

Figure 4.2: Comparison of pressure drop predicted by different models

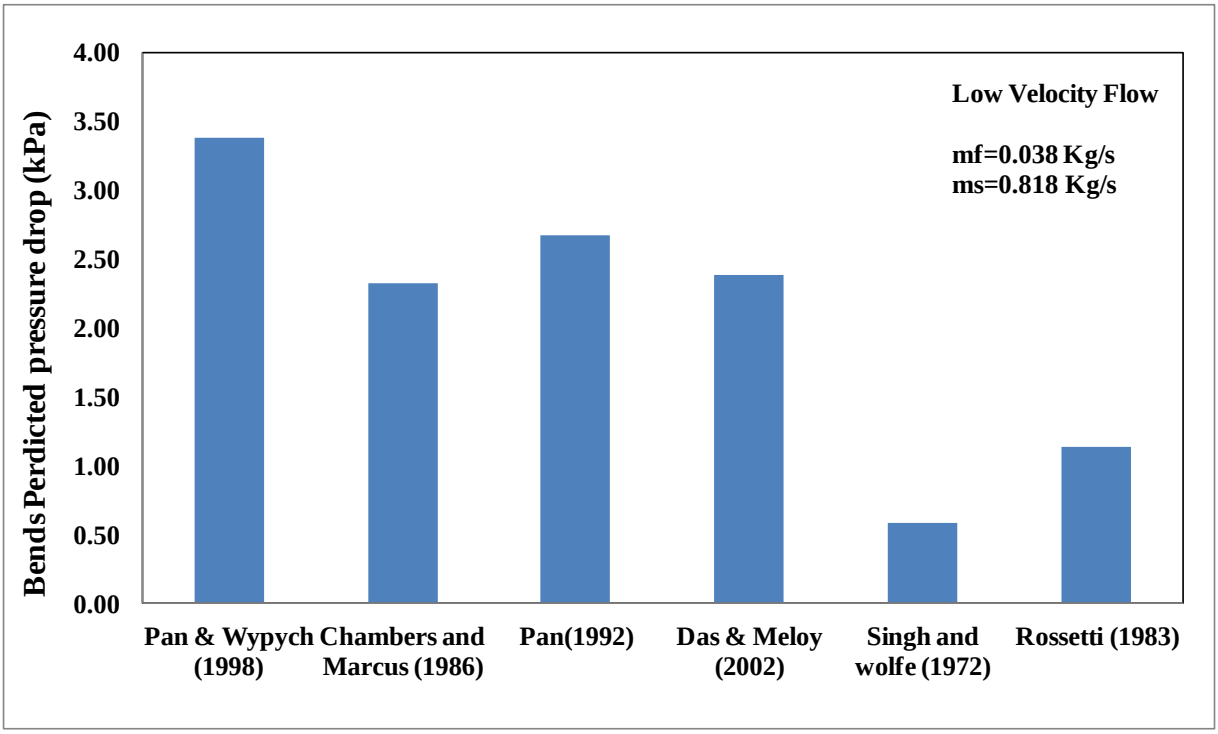

Figure 4.3: Comparison of predicted pressure drop at low velocity flow

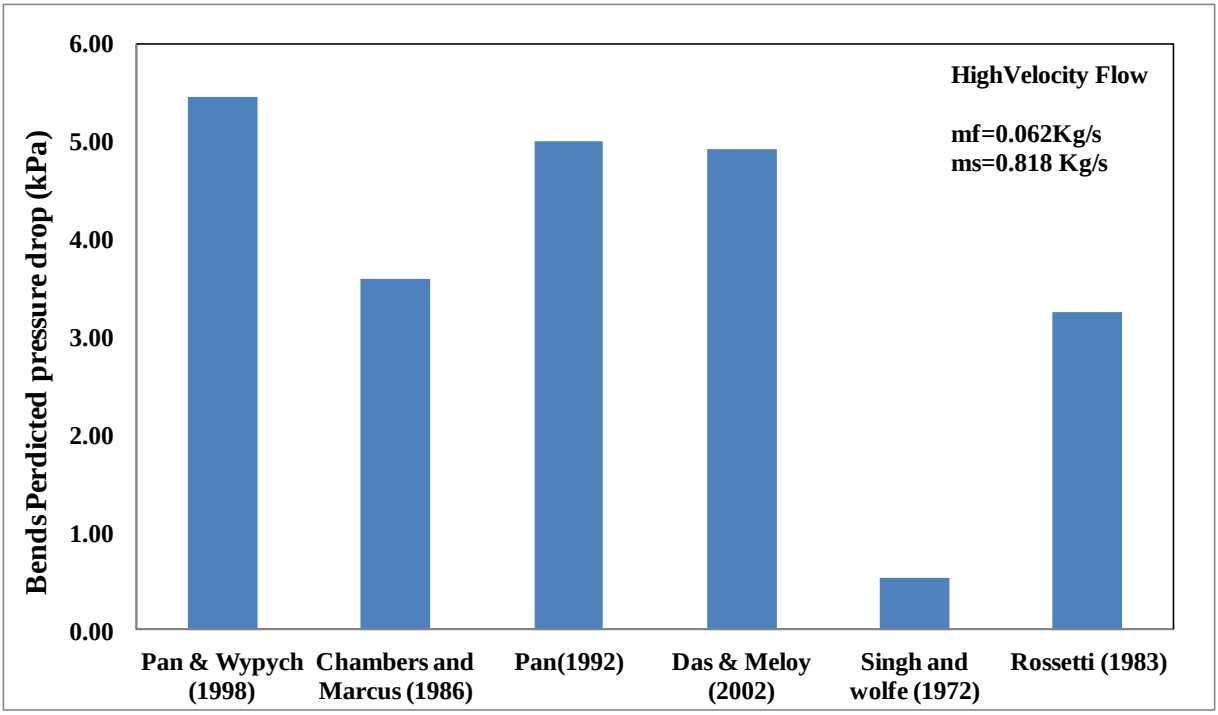

Figure 4.4: Comparison of predicted pressure drop at high velocity flow

Results and conclusions

It can be clearly seen that all models highly under-predict the value of pressure drop and it is difficult to analyse models comparison in Figure 4.1. Therefore, Figure 4.2 is zoomed view of Figure 4.1in which only bend models were compared. From Figures 4.3 and 4.4, it can be seen that models showing under-prediction at low and as well as high-velocity flow rates. So the format of Das and Meloy (2002) model can be considered for modelling purpose but as the Das and Meloy (2002) model is the modification of the Pan and Wypych (1998) model, so for modelling purpose, Pan and Wypych (1998) model format was adopted. For the modelling purpose, although all models under-predicting the pressure drop but in contrast to the experimental results Pan and Wypych model is showing good results than other models.

So on the basis of these results Pan and Wypych (1998) model is adopted for the further modelling work.

4.3 Evaluation of bend models based on University of Wollongong data

Six different bend models (Singh and Wolfe (1972), Rossetti (1983),Chambers and Marcus (1986), Pan(1992), Pan and Wypych (1998) and Das and Meloy (2002)) were used to predict the pressure drop for closely coupled bends by conveying fly ash material through 69 mm I.D. × 168 m long pipeline. The predicted pressure drop data has been compared with experimental pressure drop. The comparison of pressure drop is shown in Figure 4.5. In Figure 4.5, the "dashed" line shows the experimental pressure drop while other lines show the predicted pressure drop by different bend models. For the bend models evaluation, all models were also compared to the high and low-velocity value of conveying air. These comparisons are shown in Figure 4.6 and 4.7.

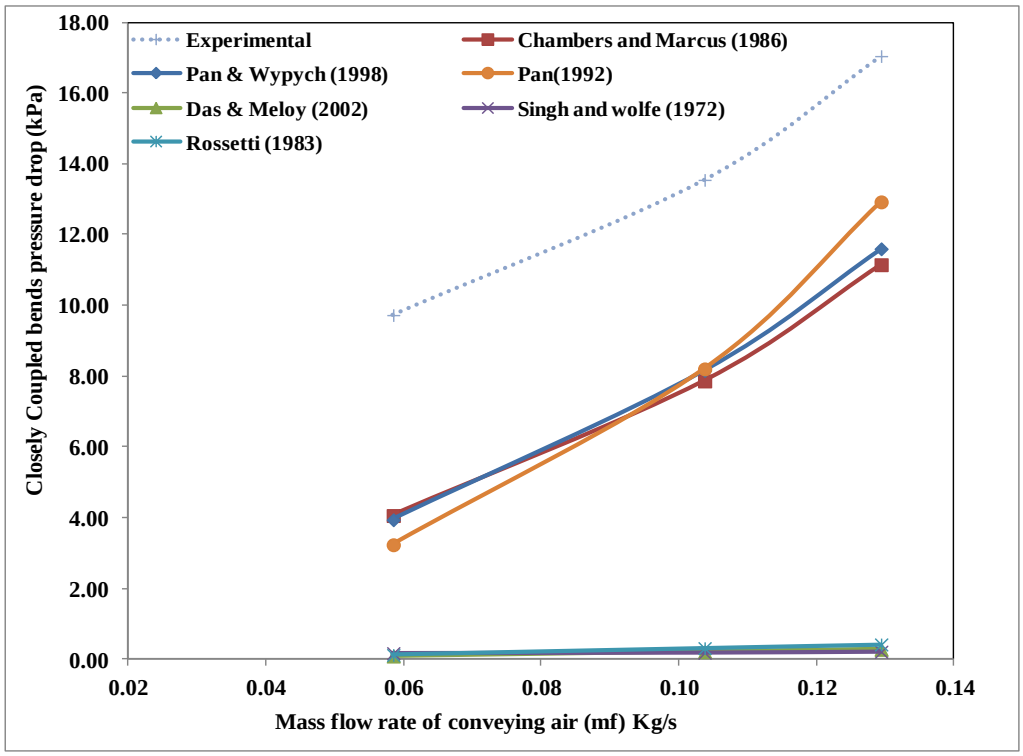

Figure 4.5: Comparison of predicted and experimental pressure drop values

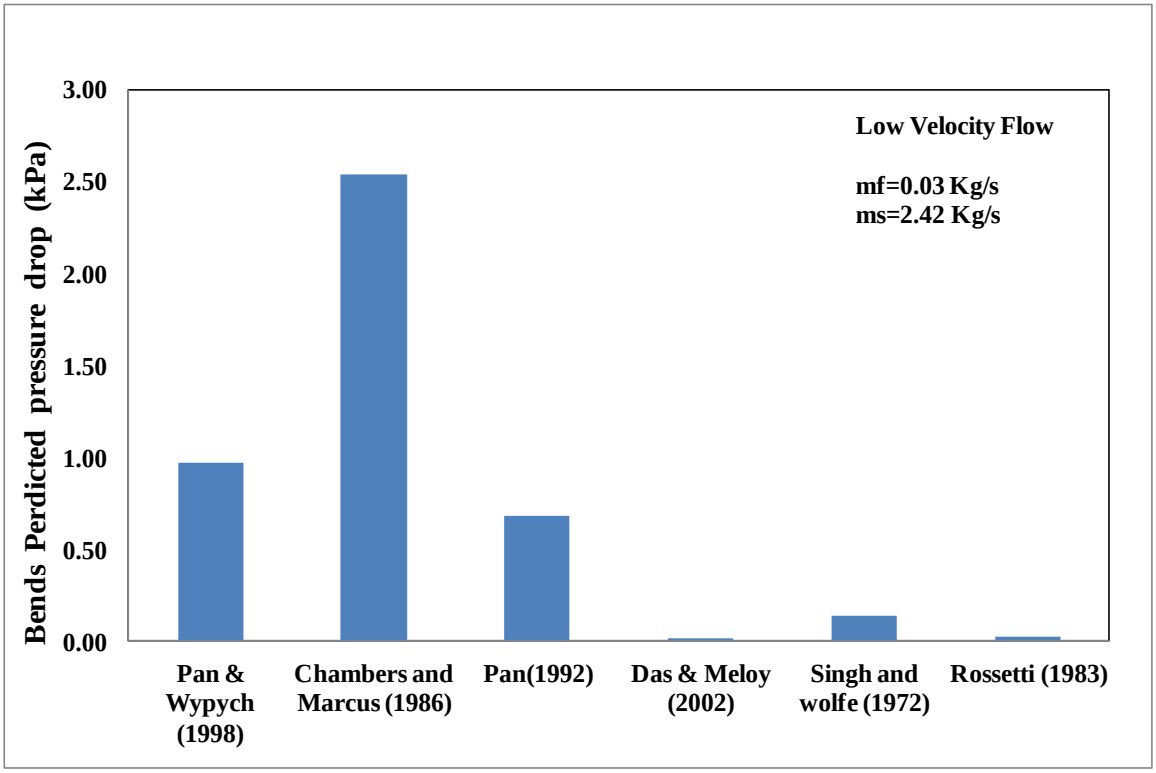

Figure 4.6: Comparison of predicted pressure drop at low velocity flow

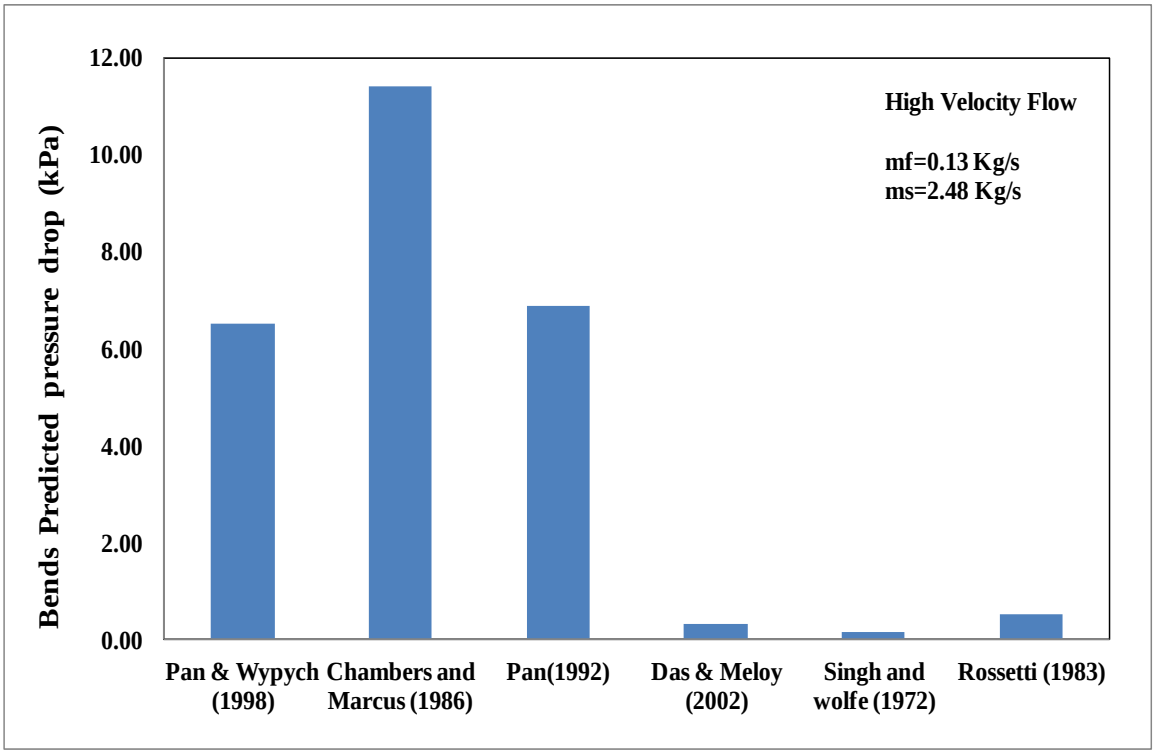

Figure 4.7: Comparison of predicted pressure drop at high velocity flow

Results and conclusions

From Figure 4.5 showed that all the models have shown under-prediction. Out of six bend models only Chambers and Marcus (1986), Pan and Wypych (1998), Pan(1992) predicted pressure drop fairly close to the experimental pressure drop data while other three models Singh and Wolfe (1972), Rossetti (1983) and Das and Meloy (2002) highly under-predict the pressure drop. Figure 4.6 showed pressure drop predicted by different models at low-velocity flow rate and Figure 4.7 showed pressure drop predicted by different models at a high-velocity flow rate. It can be seen that at both low and high-velocity flow rates pressure drops predicted by Singh and Wolfe (1972), Rossetti (1983) and Das and Meloy (2002) are very low, which is similar to the results shown in Figure 4.5.

So for the modelling purpose for the Wollongong data Chambers and Marcus (1986), Pan and Wypych (1998) can be used so to model the solid friction factor so Pan and Wypych (1998) model was chosen.

4.4 Modeling of solid friction factor

As it has been already seen that three models Chambers and Marcus (1986), Pan and Wypych (1998), Pan(1992) predicted pressure drop fairly close to the experimental pressure drop so out of these three models Pan and Wypych (1998) was selected for the modelling purpose. Pan and Wypych (1998) model as shown:

$$\lambda_{bs} = a(m^*)^b \left(Fr_f\right)^c \left(\rho_f\right)^d \tag{4.1}$$

Also, a new model has been suggested by just modifying Pan and Wypych (1998) model as Pan and Wypych (1998) does not include the material properties and also does not include the effect of bend radius. New proposed model is as follows:

$$\lambda_{bs} = a(m^*)^b (Fr_p)^c (Fr_f)^d \tag{4.2}$$

where $Fr_f = \frac{w_{fo}}{\sqrt{2Rg}}$

and $w_{fo} = \frac{d^2(\rho_p - \rho_f)g}{18\nu}$ (Stokes No.)

In the new suggested model w_{fo} consists material properties (particle size and particle density) while Froude no. of particle shows the effect material properties and radius of curvature of the bend.

For the modelling work, two models Equation 4.1 and Equation 4.2 were finalised and modelling was done for two materials (Fly ash and cement) whose properties are shown in chapter 3.

4.4.1 Modelling for Thapar University data

For Thapar data, modelling was done on 54 mm I.D. × 69 m long pipeline. A closely coupled bend was selected between two pressure transducers locations P3 and P4. Experimental work was done on cement. A similar technique was followed to find λ as was used in Wollongong data. Two models formed by using Thapar data are Equation 4.5 and Equation 4.6 as shown:

$\lambda_{bs} = 0.4212(m^*)^{-0.3331}(Fr_f)^{-0.6534}(\rho_f)^{-2.7244}$ [$R^2 = 0.880$]

(Model 3)

The above model is of the same format as Pan and Wypych (1998) model.

The New proposed model as "New model" is shown as:

$\lambda_{bs} = 2.7758(m^*)^{-0.4730}(Fr_f)^{-0.8508}(Fr_p)^{0.3345}$ [$R^2 = 0.855$]

(Model 4)

The above model includes material properties as well as the effect of radius of curvature of bend.

4.4.2 Validation of models

Model 3 and model 4 were derived from the 54 mm I.D. × 69 m long pipeline for cement material. These models were further evaluated on the Wollongong pipeline (69 mm I.D. × 168 m long pipeline) for different material (White powder) to analyse the effect of material properties. The material properties of the White powder are shown in chapter 3 and setup layout has been shown in Appendix A1.

The validation results of models are shown in Figure 4.8 and 4.9 respectively. In these Figures predicted pressure was compared with experimental pressure drop values.

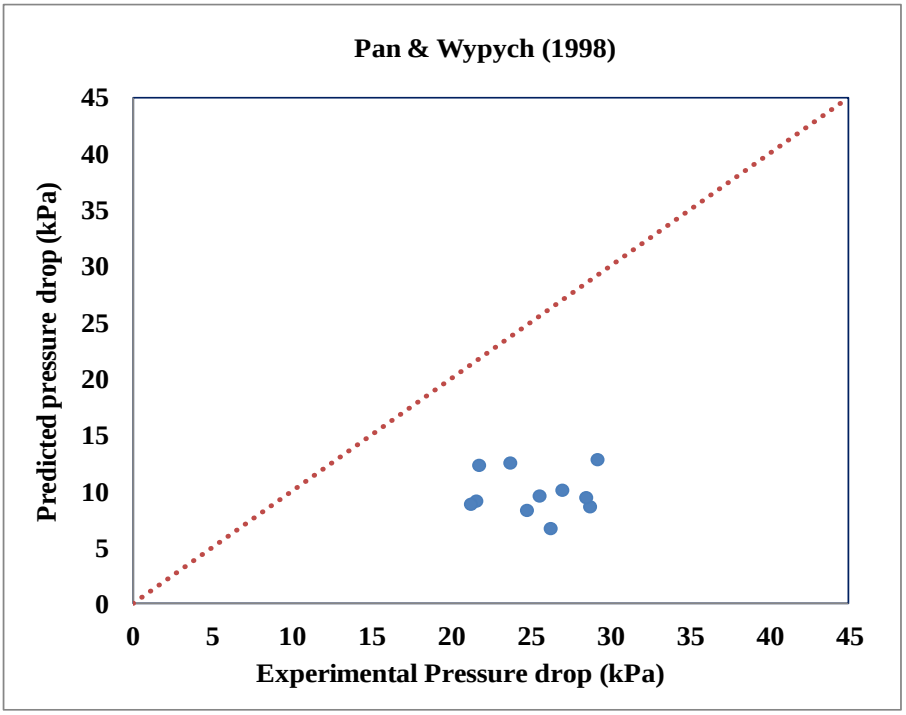

4.8: Comparison of predicted and Experimental pressure drop for Pan and Wypych (1998)

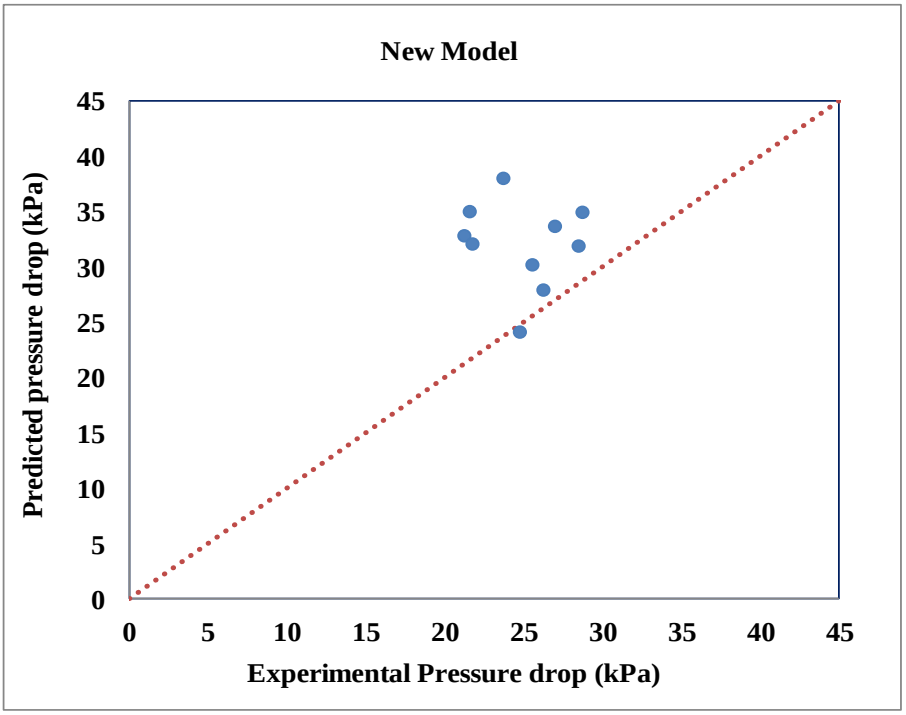

Figure 4.9: Comparison of predicted and Experimental pressure drop for New Model

For Thapar data "New model" is again showing the better prediction for pressure values. The reason is same because "New model" includes the material properties (particle size and particle density). From Figure 4.8 and 4.9 it can be seen that Pan and Wypych (1998)

model highly under-predict the pressure drop values. The range of under-predicted values is 43.33% to 74.51%. This is percentage error. “New model” showing better results, although “New model” is showing over-prediction but maximum values are close to the linear line and range of percentage of error is 2.2% to 62.8%.

After comparison of all models, it can be concluded that “New model” is valid only for a small range of conveying conditions and showing some better results as comparative to Pan and Wypych (1998) model. Also, base format of the “New model” is same as that of Pan and Wypych (1998) model and Pan and Wypych (1998) model is widely accepted for bends pressure drop predictions. In the “New model” there is just the difference of material properties (Particle size and particle density) so the “New model” predictions are better than Pan and Wypych (1998) model.

4.4.3 Modelling for University of Wollongong data

Modelling of both the data (Wollongong and Thapar) was done by using "Regression" tool in "Data Analysis" tool pack of Microsoft Excel 2007. As Mallick (2009) found "Regression" tool (Microsoft Excel 2003) more reliable than the "manual method" for modelling. For the University of Wollongong, data modelling work was done on 69 mm I.D. × 168 m long pipeline. A closely coupled bend was selected between two pressure transducers locations P10 and P11. Material conveyed was fly ash. Solution technique to find λ was based on the work of Wypych (1989).

$\lambda_{bs} = 41.758(m^*)^{-1.1906}(Fr_f)^{-2.2364}(\rho_f)^{0.5998}$ [$R^2 = 0.978$]

(Model 1)

The above model is as same as Pan and Wypych (1998) model.

New proposed model also of the same format of Pan and Wypych (1998) model just with the modification of replacement of density of fluid with Froud no. of particle.

$\lambda_{bs} = 3.237(m^*)^{-1.1906}(Fr_f)^{-2.2364}(Fr_p)^{-0.5992}$ [$R^2 = 0.978$]

(Model 2)

The above model includes material properties as well as the effect of radius of curvature of bend.

4.4.4 Validation of models

Model 1 and model 2 were derived from the 69 mm I.D. × 168 m long pipeline for fly ash material. These models were further evaluated on the new pipeline (69 mm I.D. × 148 m long pipeline) for different material (White powder) to analyse the effect of material properties.

The validation results of models are shown in Figure 4.9 and 4.10 respectively. In these Figures predicted pressure was compared with experimental pressure drop values. It can be seen that "New model" is showing the better prediction for pressure values because "New model" includes the material properties (particle size and particle density).

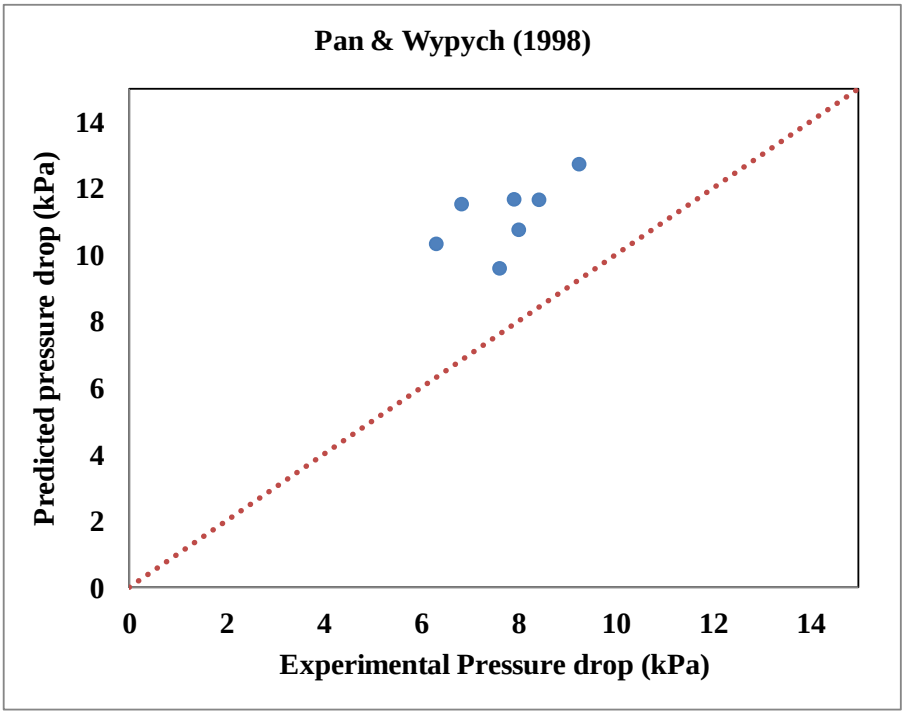

Figure 4.10: Comparison of predicted and Experimental pressure drop for Pan and Wypych (1998)

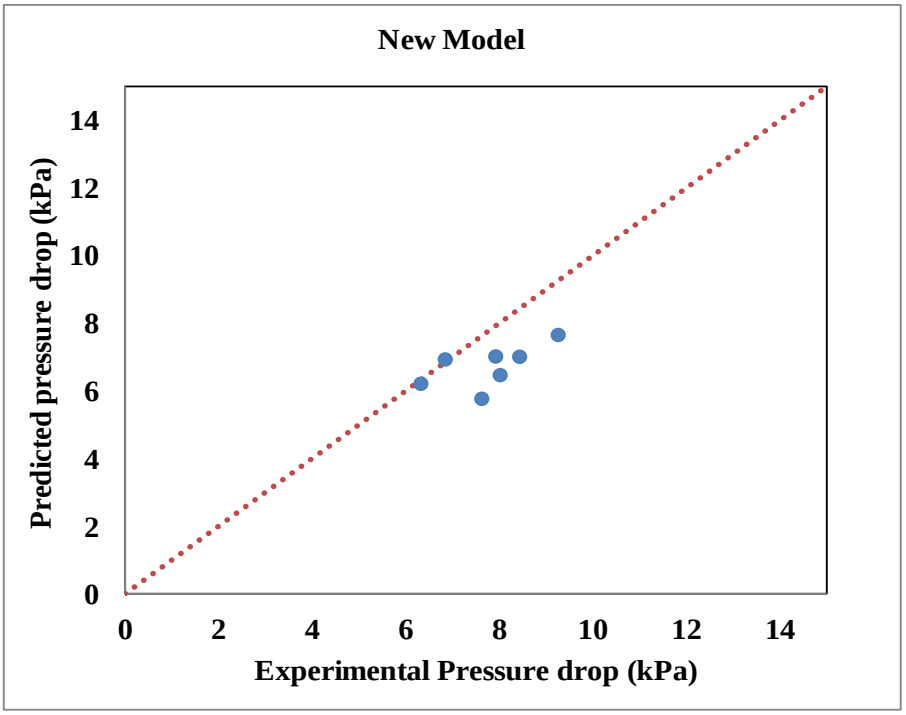

Figure 4.11: Comparison of predicted and Experimental pressure drop for New Model

In Pan and Wypych (1998) model, all value of pressure drop is over-predicted. The model over-predicted the experimental values 26.39% to 69.26 % for closely coupled bends.

"New model", under-predict the pressure drop values, but are very close to the linear line. The under-prediction range for the "New model" is 1.23% to 24%. Which results in better prediction values than the Pan and Wypych (1998).

4.5 Numerical Simulation

The computational grid generated in Ansys Fluent 15.0. For analysis of the effect of particle size distribution, three different solid phases included of different mean particle diameter and volume fraction (Table 4.1). To compare these results simulation also done on the same grid having a single solid phase of mean particle diameter d_{50} (Table 4.1). Suitable simulation parameters are selected for simulation analysis (Table 4.2). In simulation analysis, 'Phase Coupled SIMPLE' is selected for pressure-velocity coupling. For scalar parameters (momentum, turbulent kinetic energy, volume fraction etc.) First order upwind discretization is used. Stationary wall condition has been selected as a boundary condition at the pipe wall.

Table 4.1 Mean particle sizes and respective volumetric percentages of solid phases

Solid Phase	Mean particle diameter (μm)	volume %
1	11	32.91
2	27	35.24
3	98	31.39

Table 4.2 Simulation parameters

Model	Parameters
Solver type	Pressure based
Velocity formulation	Absolute
Time	Steady
Multiphase model	Eulerian
Turbulent Model	Standard k- ε (2 equation model)
Near-wall treatment	Standard wall function
Turbulent multiphase model	Dispersed
Pressure – velocity coupling	Phase Coupled SIMPLE

Experimental values of pressure drop and solid volume fraction at the inlet of pipe are taken as inlet boundary conditions for the grid. Different experimental flow conditions (solid and air mass flow rate, pressure drop) have been used for simulation. Before simulating multiphase, simulations have been done on single phase and find % error of simulation values within -15% margins. Grid independent tests also conducted on a different number of hexahedral cells (175052, 195093). It has been noted that difference in pressure drop prediction by using these two models is negligible for both single and multiphase flows.

4.5.1 Grid generation

A three-dimensional grid has been generated in Ansys Fluent 15.0 for closely coupled bends. The inlet and outlet conditions of the grid taken corresponding to the position of P3 and P4 pressure transducers. A typical grid has been shown in Figure 4.12.

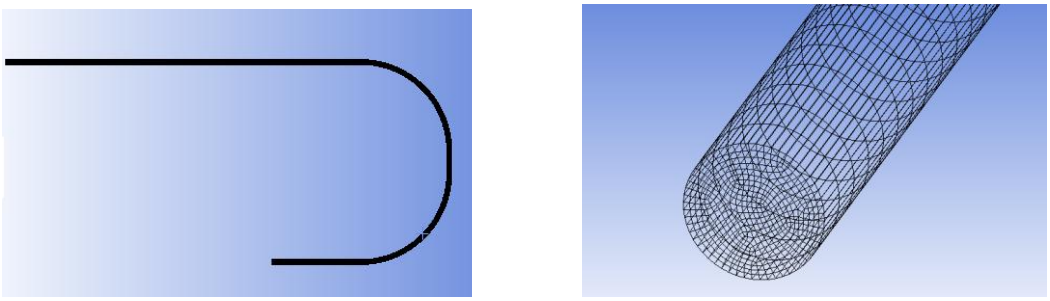

Figure 4.12: Computation grid of closely-coupled bends

The corresponding grid statistics is given below:

Volume statistics:

minimum volume (m^3) : 4.27×10^{-08} m^3

maximum volume (m^3) : 1.92×10^{-07} m^3

total volume (m^3) : 1.91×10^{-03} m^3

Face area statistics:

minimum face area (m^2) : 2.22×10^{-06} m^3

maximum face area (m^2) : 7.59×10^{-05} m^3

4.5.2 Results and discussion

Comparison of experimental and predicted pressure drop

Comparison of experimental and predicted pressure drop is shown in Figure 4.13. Comparison plot of predicted pressure drop by using particle size distribution shows better results than pressure drop predicted by using a single particle size of mean particle diameter equal to d_{50}. Although both results under predict the pressure drop but there is significantly decrease in % error by using particle size distribution (Table A2). Figure 4.13 shows that most of the predicted pressure drop points by using single particle size lie within -80% margin while for particle size distribution most of the points lie within -50% margin.

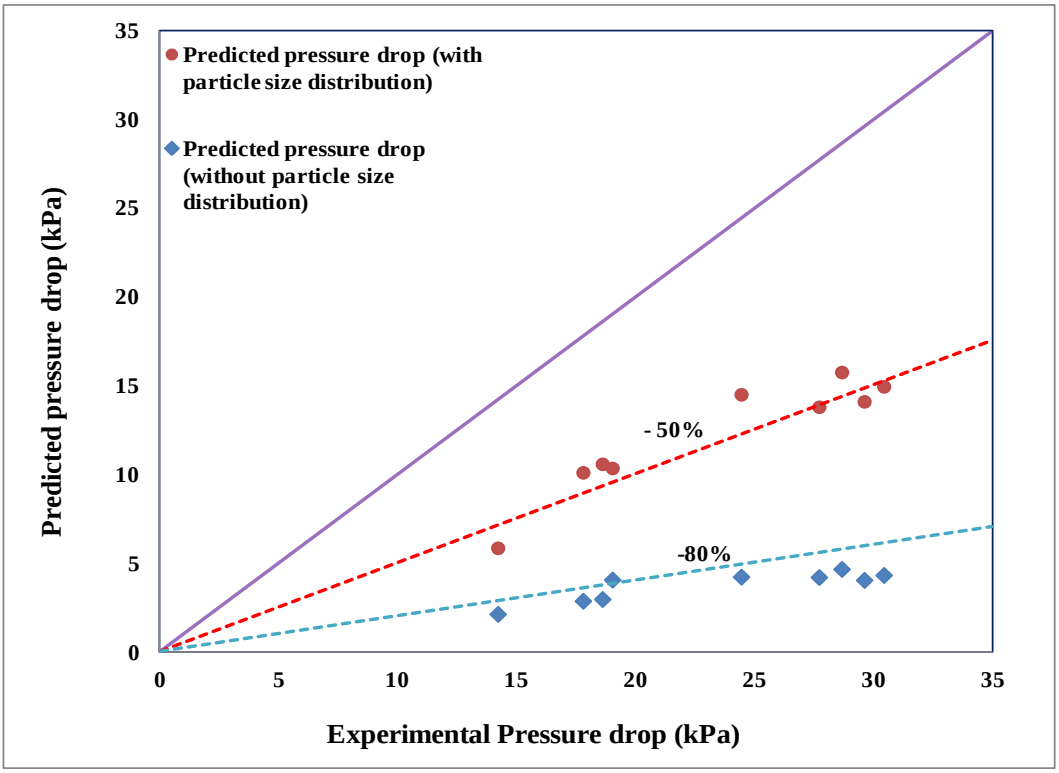

Figure 4.13: Comparison of experimental and predicted pressure drop

From Table A1, it can be clearly seen that % error range for without particle size distribution results is 78% to 86%, which is reduced to 40% to 58% by using the particle size distribution.

Solid volume fraction

The solid volume fraction of different solid phases at outlet cross-section of the 1st bend (B2) and 2nd bend (B3) are shown in Figure 4.14 and 4.15 respectively. Results show that solid volume fraction range for fine particles (d_p=11 µm) is lower than other two phases (d_p=27 µm

and d_p=98 μm). Inlet solid volume for three solid phases (d_p=11 μm, d_p=27 μm and d_p=98 μm) is 0.43%, 0.46% and 0.41%. At the outlet of the 1st bend maximum volume fraction for three solid phases (d_p=11 μm, d_p=27 μm and d_p=98 μm) becomes 8.0%, 26.6% and 27.9%. Solid volume fraction for all three phases increases after 1st bend because the maximum material was in fluidised form and due to centrifugal force particles get collected at the inner wall of the pipe. After passing 1st bend material enters 2nd bend. As bends are closely spaced so the material was not able to re-accelerate and so solid volume fraction increases further. The exception is only for course particles (d_p=98 μm), whose solid volume fraction decreases by 2% and becomes 25.1%. for other two phases (d_p=11 μm and d_p=27 μm) solid volume fraction increases up to 10.2% and 28.3% respectively.

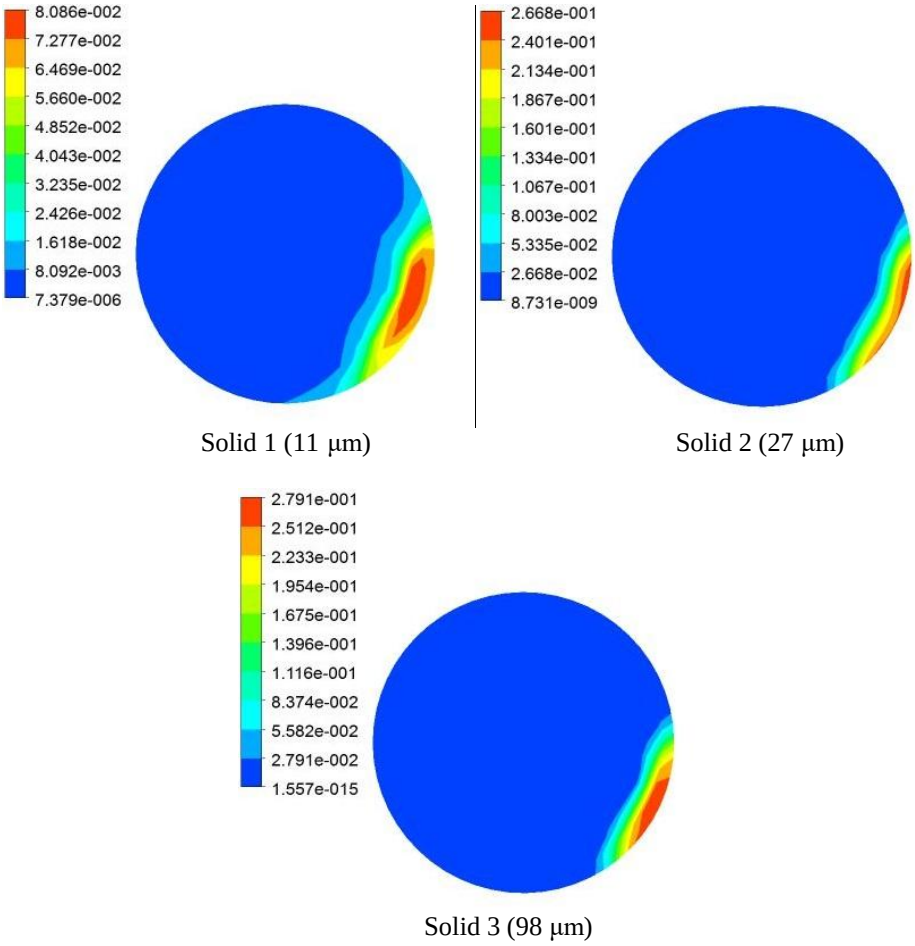

Figure 4.14: Solid volume fraction contours at the outlet of 1st bend B2 (for flow conditions m_g=0.051kg/s, m_s=1.113 kg/s)

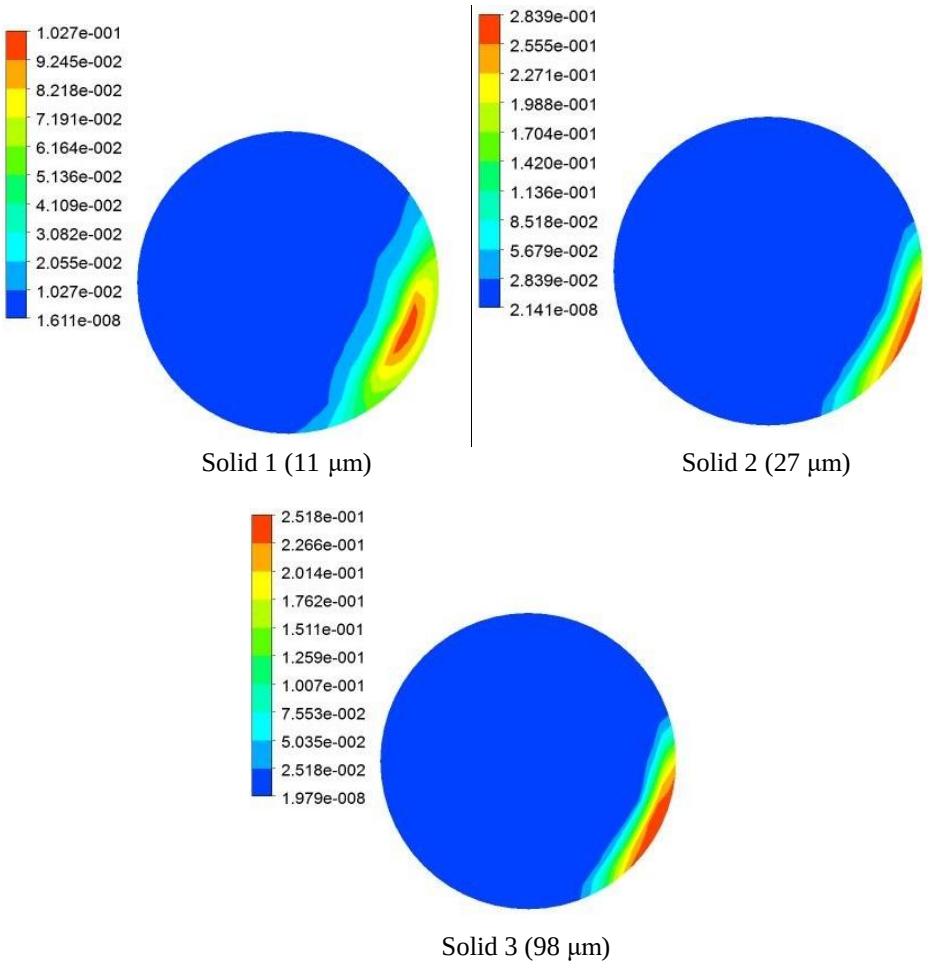

Figure 4.15: Solid volume fraction contours at the outlet of 2nd bend B3 (for flow conditions m_g = 0.051kg/s, m_s=1.113 kg/s)

Void fraction distribution

In the simulation results, void fraction at the outlet of 1st bend and 2nd bend shown in Figures 2 and Figure 3 respectively. While moving through bends, due to centrifugal force material gets collected at the outer wall of the pipe and segregation occurs. The higher void fraction at outlet cross-section of the 1st bend (0.9413 – 1.000) and outlet of the 2nd bend (0.9408-1.000) represents the dilute phase.

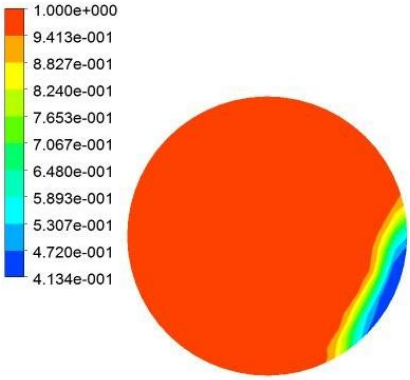

Figure 4.16: Void fraction at the outlet of 1st bend B2
(for flow conditions m_g=0.051kg/s, m_s=1.113kg/s)

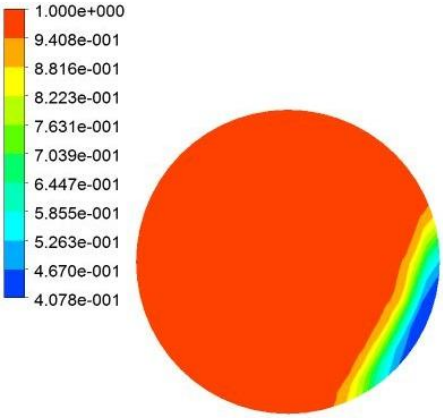

Figure 4.17: Void fraction at the outlet of 2nd bend B3
(for flow conditions m_g=0.051kg/s, m_s =1.113 kg/s)

Absolute pressure variation

To analyse the pressure variation in the closely-coupled bend along the axial direction, pressure drop predicted at different locations (Figure 4.16). From Figure 4.16, it can be clearly seen that absolute as well as local pressure gradient decreases with distance.

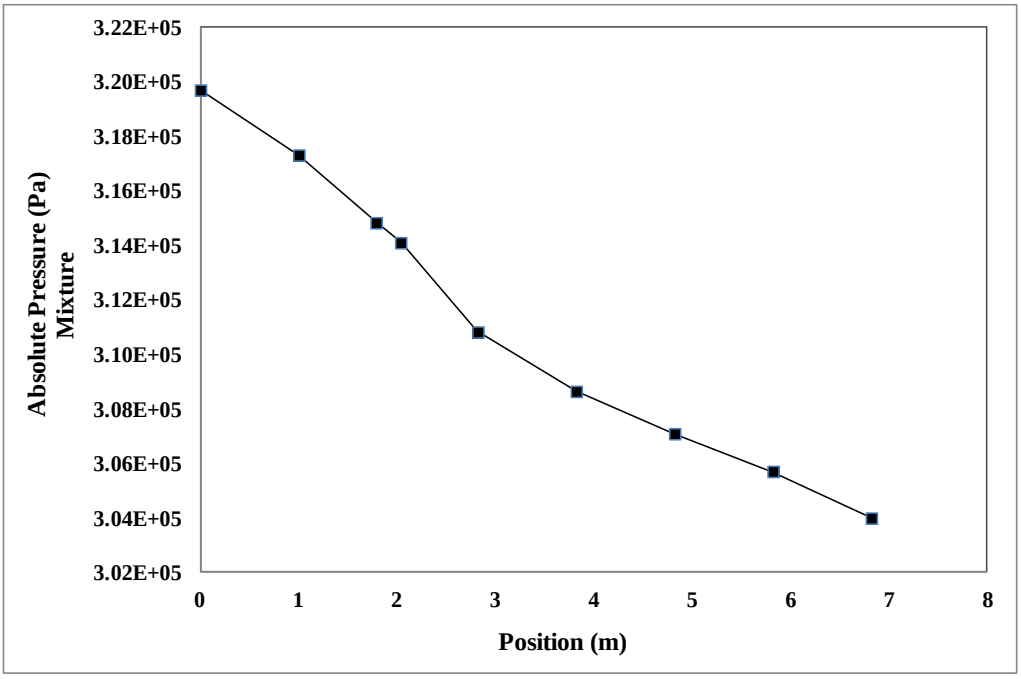

Figure 4.16 absolute pressure variations in closely coupled bends along the length of pipeline (for flow conditions m_g=0.051kg/s, m_s=1.113 kg/s)

Chapter 5

Conclusions and Future Scope of Work

5.1 Conclusions

In this study, six bend models were evaluated for accuracy in predicting the closely-coupled bend pressure drop for different materials (by using Thapar University cement data and University of Wollongong Fly ash data). Results show that none of the models were found to be accurately predicting the pressure drop for different materials. All models under-predict the pressure drop values. However, Pan and Wypych (1998), Pan (1992) and Chambers and Marcus (1986) predicted better results than other three models. A new model named as 'New Model' was introduced by modifying the Pan and Wypych (1998) model. The new proposed model includes the particle properties, which were not considered in the reference model. Modelling was done with Thapar University cement data and University of Wollongong Fly ash data. These models were validated with University of Wollongong white powder data. From validation results, it can be concluded that proposed model showing improvement in predicting the pressure drop values across closely-coupled bends.

The simulation modelling has been done on closely-coupled bends. Three solid phases of different mean particle diameter and volume fraction have been introduced. A simulation study shows that there is significantly reduction in % error when pressure drop was predicted by using particle size distribution. For single particle size, maximum points are lying within -80% range while for simulation with particle size distribution are lying -50% range.

The solid volume fraction for three solid phases has also been analysed at the outlet of 1^{st} and 2^{nd} bends. Results show that at the outlet of the 1^{st} bend solid volume fraction for all three phases increases but at the outlet of the 2^{nd} bend solid volume fraction for coarse particles (d_p=98 μm) decreases while solid volume fraction for fine particle (d_p=11 μm and d_p=27 μm) increases after the 2^{nd} bend. The main reason of this phenomenon is segregation of material. Coarser particle gets separated from fine and gets fluidised while fine particle gets denser while passing through the bends.

It needs to be stated that present experimental and simulation study does not claim to offer a complete theory of modelling of pressure drop across closely-coupled bends. The main aim of this study was to assist the engineers and research scholars involved in the study of

closely-coupled bends to provide some guidance on modelling of pressure drop by understanding the accuracies/inaccuracies of existing modelling.

5.2 Scope of further research

Although the results obtained from experimental and simulation work have contributed significantly to understand the flow phenomenon across closely-coupled bends, the following areas of investigation still require further attention:

i. Experimental work can be done to visualize the roping phenomenon in bends.
ii. Further experimental work can be carried out to calculate the particle velocity before and after the bend.

Communications

Kumar, A., Sharma, A. Simulation Analysis into Pressure Drop for Pneumatic Conveying of Fine Powders Through Closely-Coupled Bends. PGBSIA Conference 2016

References

Chambers, A.J. and Marcus, R.D., 1986. Pneumatic conveying calculations. In *Second International Conference on Bulk Materials Storage, Handling and Transportation: 1986; Preprints of Papers* (p. 49). Institution of Engineers, Australia.

Cui, J., 2009, January. Numerical Modeling of Pressure Losses Caused by Bends in Pneumatic Conveying Pipeline. In *ASME 2009 International Mechanical Engineering Congress and Exposition* (pp. 1655-1658). American Society of Mechanical Engineers.

Das, P.K. and Meloy, J.R., 2002. Effect of close-coupled bends in pneumatic conveying. *Particulate science and technology*, *20*(4), pp.253-266.

Du, J., Hu, G., Fang, Z. and Gui, W., 2015. Accelerating CFD-DEM simulation of dilute pneumatic conveying with bends. *International Journal of Fluid Machinery and Systems*, *8*(2), pp.84-93.

Hanley, K.J., Byrne, E.P. and Cronin, K., 2013. Probabilistic analysis of particle impact at a pipe bend in pneumatic conveying. *Powder technology*, *233*, pp.176-185.

Huang, G., Bryden, K.M., Vasquez, E. and Avancha, R., 2004, January. Using CFD to model coal roping phenomenon in coal transport systems. In *ASME 2004 Power Conference* (pp. 753-759). American Society of Mechanical Engineers.

Ito, H., 1960. Pressure losses in smooth pipe bends. *Journal of Basic Engineering*, *82*(1), pp.131-140.

Jones, M.G. and Williams, K.C., 2003. Solids friction factors for fluidized dense-phase conveying. *Particulate Science and Technology*, *21*(1), pp.45-56.

Klinzing, G.E., Rizk, F., Marcus, R. and Leung, L.S., 2011. *Pneumatic conveying of solids: a theoretical and practical approach* (Vol. 8). Springer Science & Business Media.

Konan, N.A., Laín, S., Simonin, O. and Sommerfeld, M., 2006, January. Comparison between euler-euler and euler-lagrange computations of gas-solid turbulent flow in a horizontal channel with different wall roughness. In *ASME 2006 2nd Joint US-European Fluids Engineering Summer Meeting Collocated With the 14th International Conference on Nuclear Engineering* (pp. 617-625). American Society of Mechanical Engineers.

Kuan, B.T. and Schwarz, M.P., 2003, January. CFD simulation of single-phase and dilute particulate turbulent flows in 90 duct bends. In *ASME/JSME 2003 4th Joint Fluids Summer Engineering Conference* (pp. 1901-1908). American Society of Mechanical Engineers.

Mainwaring, N.J. and Reed, A.R., 1987. Permeability and air retention characteristics of bulk solid materials in relation to modes of dense phase pneumatic conveying. *Bulk Solids Handling*, *7*(3), pp.415-425.

Mallick, S.S. and Wypych, P.W., 2009. Minimum transport boundaries for pneumatic conveying of powders. *Powder Technology*, *194*(3), pp.181-186.

Mallick, S.S. and Wypych, P.W., 2011. On improving scale-up procedures for dense-phase pneumatic conveying of powders. *Particulate Science and Technology*, *29*(5), pp.407-427.

Mallick, S.S., 2009. Modelling of fluidised dense-phase pneumatic conveying of powders.

McGlinchey, D., Cowell, A., Knight, E.A., Pugh, J.R., Mason, A. and Foster, B., 2007. Bend pressure drop predictions using the Euler-Euler model in dense phase pneumatic conveying. *Particulate Science and Technology*, *25*(6), pp.495-506.

Middha, P., Balakin, B.V., Leirvaag, L., Hoffmann, A.C. and Kosinski, P., 2013. PEPT—A novel tool for investigation of pneumatic conveying. *Powder technology*, *237*, pp.87-96.

Mills, D. and Mason, J.S., 1985, May. The influence of bend geometry on pressure drop in pneumatic conveying system pipelines. In *Proceedings of 10th Annual Conference on Powder and Bulk Solids Handling and Processing. Rosemont. Illinois* (pp. 203-214).

Mills, D., 2003. *Pneumatic conveying design guide*. Butterworth-Heinemann.

Pan, R. and Wypych, P.W., 1998, September. Dilute and dense phase pneumatic conveying of fly ash. In *Proceedings of the 6th International Conference on Bulk Materials Storage and Transportation, Wollongong, NSW, Australia* (pp. 183-189).

Pan, R., 1992. Improving scale-up procedures for the design of pneumatic conveying systems.

Ratnayake, C., 2005. A comprehensive scaling up technique for pneumatic transport systems.

Rossetti, S.J., 1983. Concepts and criteria for gas-solids flow. *Handbook of Fluids in Motion. Michigan: Ann Arbor Science*, p.1202.

Schuchart, P., 1968. Widerstandsgesetze beim pneumatischen Transport in Rohrkrümmern. *Chemie Ingenieur Technik*, *40*(21-22), pp.1060-1067.

Singh, B. and Wolfe, R.R., 1972. Pressure losses due to bends in pneumatic forage handling. *Transactions of the ASAE*, *15*(2), pp.246-0248.

Tripathi, N., Sharma, A., Mallick, S.S. and Wypych, P.W., 2015. Energy loss at bends in the pneumatic conveying of fly ash. *Particuology*, *21*, pp.65-73.

Tu, J.Y. and Fletcher, C.A.J., 1995. Numerical computation of turbulent gas-solid particle flow in a 90° bend. *AIChE Journal*, *41*(10), pp.2187-2197.

Williams, K.C. and Jones, M.G., 2004, July. Numerical model velocity profile of fluidized dense phase pneumatic conveying. In *Proceedings of 8th International Conference on Bulk Materials Storage and Transportation* (pp. 354-358).

Wypych, P.W. and Arnold, P.C., 1989. Plug-phase pneumatic transportation of bulk solids and the importance of blow tank air injection. *Powder Handling and Processing*, *1*(3), pp.271-275.

Wypych, P.W. and Hauser, G., 1990. Design considerations for low-velocity conveying systems & pipelines. In *Pneumatech 4, Int. Conf. on Pneumatic Conveying Technology* (pp. 241-260).

Wypych, P.W., 1989. Pneumatic conveying of bulk solids.

Wypych, P.W., 2006. Course notes written on pneumatic conveying of bulk solids and dust control. *University of Wollongong*.

Appendix-A1

Table A1.1 Closely-coupled bend data for Model 1																		
Exp. No.	**mf**	**ms**	**m***	**P3**	**P4**	**ΔP**	**ρ air**	**Pipe dia d**	**Particle dia dp**	**ρ particle**	**V4**	**Fr**	**Re**	**λs**	**log10**	**log10**	**log10**	**log10**
	kg/s	**kg/s**		**kPa**	**kPa**	**kPa**	**kg/m3**	**m**	**μm**	**kg/m3**	**m/s**	**at bend outlet**	**at bend outlet**		**λs**	**m***	**Fr**	**ρ**
1	0.09	5.10	55.26	112.4	99.7	12.8	1.28	0.069	30	2300	10.3	12.6	16460	0.0025	-2.61	1.11	1.39	0.31
2	0.07	2.74	39.29	61.6	52.2	9.3	1.30	0.069	30	2300	10.2	12.4	21250	0.0025	-2.60	1.31	1.26	0.28
3	0.07	4.78	66.69	103.0	90.3	12.7	1.31	0.069	30	2300	8.4	10.2	14061	0.0025	-2.60	1.34	1.26	0.28
4	0.08	2.49	30.52	65.3	55.2	10.1	1.33	0.069	30	2300	11.7	14.3	23983	0.0023	-2.64	1.30	1.30	0.31
5	0.08	3.96	48.41	86.7	74.9	11.7	1.34	0.069	30	2300	10.4	12.7	18939	0.0025	-2.61	1.47	1.18	0.28
6	0.02	2.38	103.18	65.6	54.7	10.9	1.36	0.069	30	2300	3.3	4.0	6823	0.0025	-2.59	1.48	1.15	0.27
7	0.11	2.35	21.82	70.2	59.2	11.0	1.37	0.069	30	2300	15.1	18.3	30043	0.0025	-2.61	1.59	1.09	0.26
8	0.05	5.29	106.71	88.6	77.0	11.7	1.37	0.069	30	2300	6.3	7.6	11237	0.0029	-2.54	1.69	1.02	0.25
9	0.06	2.85	48.77	59.8	50.1	9.7	1.39	0.069	30	2300	8.7	10.6	18363	0.0042	-2.37	1.84	0.87	0.25
10	0.09	3.98	44.97	90.5	78.1	12.3	1.40	0.069	30	2300	11.1	13.5	19776	0.0086	-2.07	1.96	0.68	0.26
11	0.11	2.21	20.50	71.3	59.9	11.4	1.42	0.069	30	2300	15.1	18.3	29901	0.0102	-1.99	2.01	0.61	0.27
12	0.08	5.19	63.73	106.1	92.5	13.6	1.42	0.069	30	2300	9.5	11.5	15620	0.0023	-2.64	1.44	1.26	0.36
13	0.13	2.48	19.77	84.9	72.0	12.8	1.44	0.069	30	2300	16.3	19.8	30095	0.0021	-2.68	1.56	1.19	0.34
14	0.04	2.79	69.02	56.6	46.9	9.7	1.46	0.069	30	2300	6.1	7.5	13229	0.0021	-2.69	1.65	1.13	0.33
15	0.07	4.17	59.51	83.2	71.5	11.7	1.46	0.069	30	2300	9.1	11.1	16884	0.0021	-2.68	1.68	1.10	0.32
16	0.03	2.41	91.05	62.5	51.7	10.8	1.48	0.069	30	2300	3.9	4.7	8141	0.0023	-2.64	1.77	1.04	0.31
17	0.09	2.62	29.62	68.6	57.6	11.0	1.49	0.069	30	2300	12.5	15.2	25229	0.0025	-2.60	1.81	1.02	0.31

18	0.10	3.76	36.27	96.4	82.8	13.5	1.50	0.069	30	2300	12.7	15.4	22013	0.0031	-2.52	1.93	0.92	0.30
19	0.13	5.01	38.74	131.2	114.2	17.0	1.51	0.069	30	2300	14	16.4	20054	0.0045	-2.35	2.01	0.8	0.29
20	0.04	5.77	145.59	92.0	79.4	12.6	1.51	0.069	30	2300	4.9	6.0	8740.8	0.0018	-2.73	1.59	1.22	0.41
21	0.06	4.87	76.40	98.3	84.7	13.6	1.53	0.069	30	2300	7.7	9.4	13273	0.0018	-2.75	1.74	1.1	0.38
22	0.15	1.98	12.92	82.9	69.0	13.9	1.56	0.069	30	2300	20	24.7	38082	0.002	-2.69	1.8	1.06	0.36
23	0.11	2.37	22.03	72.5	60.2	12.3	1.57	0.069	30	2300	15	18.2	29686	0.002	-2.63	1.82	1.01	0.36
24	0.07	4.19	64.17	81.5	69.2	12.3	1.57	0.069	30	2300	8.6	10.5	16154	0.003	-2.57	1.88	0.97	0.34
25	0.05	4.28	84.91	77.5	65.5	12.0	1.59	0.069	30	2300	6.8	8.3	13044	0.003	-2.58	2.03	0.88	0.33
26	0.13	3.44	27.24	106.6	90.6	16.0	1.60	0.069	30	2300	15	18.0	24703	0.003	-2.48	2.16	0.78	0.33
27	0.04	3.90	102.86	74.5	62.2	12.3	1.61	0.069	30	2300	5.2	6.3	10205	0.002	-2.65	1.34	1.26	0.28

Table A1.2 Closely-coupled bend for Model 2																			
Exp. No.	**mf**	**ms**	**m***	**P3**	**P4**	**ΔP**	**ρ air**	**Pipe dia d**	**Particle dia dp**	**ρ particle**	**V4**	**Fr**	**Re**	**wfo**	**Fr p**	**λs**	**log10**	**log10**	**log10**	**log10**
	kg/s	**kg/s**		**kPa**	**kPa**	**kPa**	**kg/m3**	**m**	**μm**	**kg/m3**	**m/s**	**at bend outlet**	**at bend outlet**				**λs**	**m***	**Fr**	**Fr p**
1	0.15	1.98	12.92	82.9	69.0	13.9	2.023	0.069	30	2300	20.3	24.65	38082	0.031	0.007	0.002	-2.61	1.11	1.39	-2.16
2	0.11	2.21	20.50	71.3	59.9	11.4	1.915	0.069	30	2300	15.1	18.32	29901	0.032	0.007	0.002	-2.60	1.31	1.26	-2.14
3	0.11	2.37	22.03	72.5	60.2	12.3	1.919	0.069	30	2300	15.0	18.23	29686	0.032	0.007	0.003	-2.60	1.34	1.26	-2.14
4	0.13	2.48	19.77	84.9	72.0	12.8	2.060	0.069	30	2300	16.3	19.83	30095	0.030	0.007	0.002	-2.64	1.30	1.30	-2.17
5	0.09	2.62	29.62	68.6	57.6	11.0	1.888	0.069	30	2300	12.5	15.24	25229	0.033	0.007	0.002	-2.61	1.47	1.18	-2.13
6	0.08	2.49	30.52	65.3	55.2	10.1	1.859	0.069	30	2300	11.7	14.27	23983	0.033	0.008	0.003	-2.59	1.48	1.15	-2.12
7	0.07	2.74	39.29	61.6	52.2	9.3	1.824	0.069	30	2300	10.2	12.40	21250	0.034	0.008	0.002	-2.61	1.59	1.09	-2.11
8	0.058	2.85	48.77	59.8	50.1	9.7	1.799	0.069	30	2300	8.7	10.57	18363	0.035	0.008	0.003	-2.54	1.69	1.02	-2.11
9	0.040	2.79	69.02	56.6	46.9	9.7	1.761	0.069	30	2300	6.1	7.45	13229	0.035	0.008	0.004	-2.37	1.84	0.87	-2.10
10	0.026	2.41	91.05	62.5	51.7	10.8	1.818	0.069	30	2300	3.9	4.74	8141	0.034	0.008	0.009	-2.07	1.96	0.68	-2.11
11	0.023	2.38	103.2	65.6	54.7	10.9	1.853	0.069	30	2300	3.3	4.05	6823	0.033	0.008	0.010	-1.99	2.01	0.61	-2.12
12	0.126	3.44	27.24	106.6	90.6	16.0	2.280	0.069	30	2300	14.8	18.02	24703	0.027	0.006	0.002	-2.64	1.44	1.26	-2.21
13	0.104	3.76	36.27	96.4	82.8	13.5	2.188	0.069	30	2300	12.7	15.41	22013	0.028	0.006	0.002	-2.68	1.56	1.19	-2.19
14	0.088	3.98	44.97	90.5	78.1	12.3	2.132	0.069	30	2300	11.1	13.49	19776	0.029	0.007	0.002	-2.69	1.65	1.13	-2.18
15	0.08	3.96	48.41	86.7	74.9	11.7	2.094	0.069	30	2300	10.4	12.69	18939	0.030	0.007	0.002	-2.68	1.68	1.10	-2.17
16	0.07	4.17	59.51	83.2	71.5	11.7	2.053	0.069	30	2300	9.1	11.09	16884	0.030	0.007	0.002	-2.64	1.77	1.04	-2.17
17	0.07	4.19	64.17	81.5	69.2	12.3	2.025	0.069	30	2300	8.6	10.47	16154	0.031	0.007	0.003	-2.60	1.81	1.02	-2.16
18	0.05	4.28	84.91	77.5	65.5	12.0	1.982	0.069	30	2300	6.8	8.27	13044	0.031	0.007	0.003	-2.52	1.93	0.92	-2.15
19	0.04	3.9	103	74.5	62.2	12.3	1.943	0.069	30	2300	5.2	6.34	10205	0.032	0.007	0.004	-2.35	2.01	0.80	-2.14
20	0.13	5.01	38.7	131.2	114.2	17.0	2.56	0.069	30	2300	14	16.43	20054	0.024	0.005	0.002	-2.73	1.59	1.22	-2.26
21	0.09	5.1	55.3	112.4	99.7	12.8	2.388	0.069	30	2300	10	12.57	16460	0.026	0.006	0.002	-2.75	1.74	1.10	-2.23

22	0.08	5.19	63.7	106.1	92.5	13.6	2.303	0.069	30	2300	9.5	11.51	15620	0.027	0.006	0.002	-2.69	1.80	1.06	-2.22
23	0.07	4.78	66.7	103.0	90.3	12.7	2.276	0.069	30	2300	8.4	10.24	14061	0.027	0.006	0.002	-2.63	1.82	1.01	-2.21
24	0.06	4.87	76.4	98.3	84.7	13.6	2.21	0.069	30	2300	7.7	9.38	13273	0.028	0.006	0.003	-2.57	1.88	0.97	-2.20
25	0.05	5.29	107	88.6	77.0	11.7	2.118	0.069	30	2300	6.3	7.61	11237	0.029	0.007	0.003	-2.58	2.03	0.88	-2.18
26	0.04	5.77	146	92.0	79.4	12.6	2.147	0.069	30	2300	4.9	6.00	8740.8	0.029	0.007	0.003	-2.48	2.16	0.78	-2.19
27	0.11	2.35	21.8	70.2	59.2	11.0	1.907	0.069	30	2300	15	18.33	30043	0.033	0.007	0.002	-2.65	1.34	1.26	-2.13

Table A1.3 Closely-coupled bend data for model 3

Exp. No.	mf	ms	m*	P3	P4	ΔP	ρ air	Pipe dia d	Particle dia dp	ρ particle	V4	Fr	Re	λs	log10	log10	log10	log10
	kg/s	kg/s		kPa	kPa	kPa	kg/m3	m	μm	kg/m3	m/s	at bend outlet	at bend outlet		λs	m*	Fr	ρ
1	0.035	0.836	23.91	29.70	11.93	17.77	1.345	0.054	17	2950	11.3	15.6	25071	0.009	-2.07	1.38	1.19	0.13
2	0.040	0.293	7.39	18.30	3.81	14.49	1.249	0.054	17	2950	13.9	19.1	33030	0.016	-1.79	0.87	1.28	0.10
3	0.055	0.802	14.53	41.38	19.77	21.61	1.439	0.054	17	2950	16.8	23.0	34636	0.007	-2.14	1.16	1.36	0.16
4	0.026	0.770	30.06	30.26	16.40	13.86	1.398	0.054	17	2950	8.0	11.0	17000	0.010	-1.99	1.48	1.04	0.15
5	0.025	0.724	28.78	26.50	11.64	14.87	1.342	0.054	17	2950	8.2	11.2	18140	0.011	-1.94	1.46	1.05	0.13
6	0.025	0.591	23.74	25.83	11.64	14.18	1.342	0.054	17	2950	8.1	11.1	17951	0.013	-1.87	1.38	1.05	0.13
7	0.062	0.818	13.16	46.24	21.12	25.11	1.455	0.054	17	2950	18.7	25.6	38149	0.007	-2.13	1.12	1.41	0.16
8	0.051	0.979	19.16	46.20	21.55	24.66	1.460	0.054	17	2950	15.3	21.0	31136	0.007	-2.13	1.28	1.32	0.16
9	0.051	0.957	18.77	47.30	22.89	24.42	1.476	0.054	17	2950	15.1	20.7	30402	0.008	-2.12	1.27	1.32	0.17
10	0.025	0.629	24.96	28.23	12.28	15.95	1.349	0.054	17	2950	8.1	11.2	17951	0.014	-1.85	1.40	1.05	0.13
11	0.038	0.818	21.64	34.96	10.32	24.64	1.326	0.054	17	2950	12.4	17.1	27905	0.011	-1.96	1.34	1.23	0.12
12	0.026	0.693	27.14	30.62	14.16	16.47	1.372	0.054	17	2950	8.1	11.2	17617	0.013	-1.88	1.43	1.05	0.14
13	0.051	1.113	21.94	50.67	22.02	28.65	1.465	0.054	17	2950	15.1	20.8	30689	0.008	-2.11	1.34	1.32	0.17
14	0.033	0.361	11.08	22.83	5.49	17.34	1.269	0.054	17	2950	11.2	15.4	26241	0.020	-1.71	1.04	1.19	0.10
15	0.035	0.872	25.06	34.84	7.94	26.90	1.298	0.054	17	2950	11.7	16.1	26809	0.012	-1.92	1.40	1.21	0.11
16	0.052	0.865	16.76	47.21	19.52	27.69	1.436	0.054	17	2950	15.7	21.6	32513	0.009	-2.03	1.22	1.33	0.16
17	0.034	1.065	31.68	40.25	13.67	26.58	1.366	0.054	17	2950	10.7	14.8	23386	0.011	-1.98	1.50	1.17	0.14
18	0.047	1.185	25.13	51.74	21.32	30.42	1.457	0.054	17	2950	14.1	19.4	28834	0.008	-2.08	1.40	1.29	0.16

Table A1.5: Summary output of Regression Analysis for Model 1								
SUMMARY OUTPUT								
Regression Statistics								
Multiple R	0.989276114							
R Square	**0.978667229**							
Adjusted R Square	0.975884694							
Standard Error	0.027750983							
Observations	27							
ANOVA								
	df	*SS*	*MS*	*F*	*Significance F*			
Regression	3	0.812591622	0.270863874	351.717807	2.37852E-19			
Residual	23	0.017712692	0.000770117					
Total	26	0.830304313						
	Coefficients	*Standard Error*	*t Stat*	*P-value*	*Lower 95%*	*Upper 95%*	*Lower 95.0%*	*Upper 95.0%*
Intercept	**1.62074578**	0.198795787	8.152817542	3.09542E-08	1.209505367	2.031986199	1.209505367	2.031986199
log m	**-1.1906426**	0.076909048	-15.48117766	1.17845E-13	-1.34974112	-1.031544147	-1.34974112	-1.031544147
log ρ	**0.59980992**	0.200435223	2.992537487	0.00650323	0.185178071	1.014441765	0.185178071	1.014441765
log Fr	**-2.2364224**	0.107863909	-20.73374149	2.20153E-16	-2.459555908	-2.013288916	-2.459555908	-2.013288916

Table A1.6: Summary output of Regression Analysis for Model 2								
SUMMARY OUTPUT								
Regression Statistics								
Multiple R	0.989275857							
R Square	**0.978666721**							
Adjusted R Square	0.975884119							
Standard Error	0.027751313							
Observations	27							
ANOVA								
	df	*SS*	*MS*	*F*	*Significance F*			
Regression	3	0.8125912	0.270863733	351.7092448	2.37918E-19			
Residual	23	0.017713114	0.000770135					
Total	26	0.830304313						
	Coefficients	*Standard Error*	*t Stat*	*P-value*	*Lower 95%*	*Upper 95%*	*Lower 95.0%*	*Upper 95.0%*
Intercept	**0.51016913**	0.298077035	1.711534514	0.100436828	-0.10645019	1.126788457	-0.10645019	1.126788457
log m	**-1.1906328**	0.076908829	-15.48109438	1.17859E-13	-1.349730867	-1.031534801	-1.349730867	-1.031534801
log Fr	**-2.2364082**	0.107863489	-20.73369052	2.20165E-16	-2.459540823	-2.013275572	-2.459540823	-2.013275572
log Fr p	**-0.5992368**	0.200252222	-2.992410281	0.006505171	-1.013490089	-0.184983527	-1.013490089	-0.184983527

Table A1.7: Summary output of Regression Analysis for Model 3								
SUMMARY OUTPUT								
Regression Statistics								
Multiple R	0.938481							
R Square	**0.880746**							
Adjusted R Square	0.855192							
Standard Error	0.048933							
Observations	18							
ANOVA								
	df	*SS*	*MS*	*F*	*Significance F*			
Regression	3	0.247581	0.082527	34.46558	1.02E-06			
Residual	14	0.033523	0.002394					
Total	17	0.281103						
	Coefficients	*Standard Error*	*t Stat*	*P-value*	*Lower 95%*	*Upper 95%*	*Lower 95.0%*	*Upper 95.0%*
Intercept	**-0.3755**	0.273849	-1.37119	0.191896	-0.96285	0.211849	-0.96285	0.211849
log m	**-0.33319**	0.119337	-2.79199	0.014406	-0.58914	-0.07724	-0.58914	-0.07724
log ρ	**-2.72442**	0.82809	-3.29001	0.005368	-4.5005	-0.94834	-4.5005	-0.94834
log Fr	**-0.6534**	0.177959	-3.67163	0.002515	-1.03509	-0.27172	-1.03509	-0.27172

Table A1.8: Summary output of Regression Analysis for Model 4								
SUMMARY OUTPUT								
Regression Statistics								
Multiple R	0.924468397							
R Square	**0.854641817**							
Adjusted R Square	0.823493635							
Standard Error	0.048424572							
Observations	18							
ANOVA								
	df	*SS*	*MS*	*F*	*Significance F*			
Regression	3	0.193021	0.06434	27.43794	4.02E-06			
Residual	14	0.032829	0.002345					
Total	17	0.22585						
	Coefficients	*Standard Error*	*t Stat*	*P-value*	*Lower 95%*	*Upper 95%*	*Lower 95.0%*	*Upper 95.0%*
Intercept	**0.4433975**	1.462295	0.30322	0.766181	-2.69291	3.579708	-2.69291	3.579708
log m	**-0.473059238**	0.099494	-4.75465	0.000308	-0.68645	-0.25967	-0.68645	-0.25967
log Fr	**-0.850836713**	0.137567	-6.18491	2.37E-05	-1.14589	-0.55579	-1.14589	-0.55579
log Fr p	**0.334546711**	0.685872	0.487769	0.633264	-1.1365	1.805595	-1.1365	1.805595

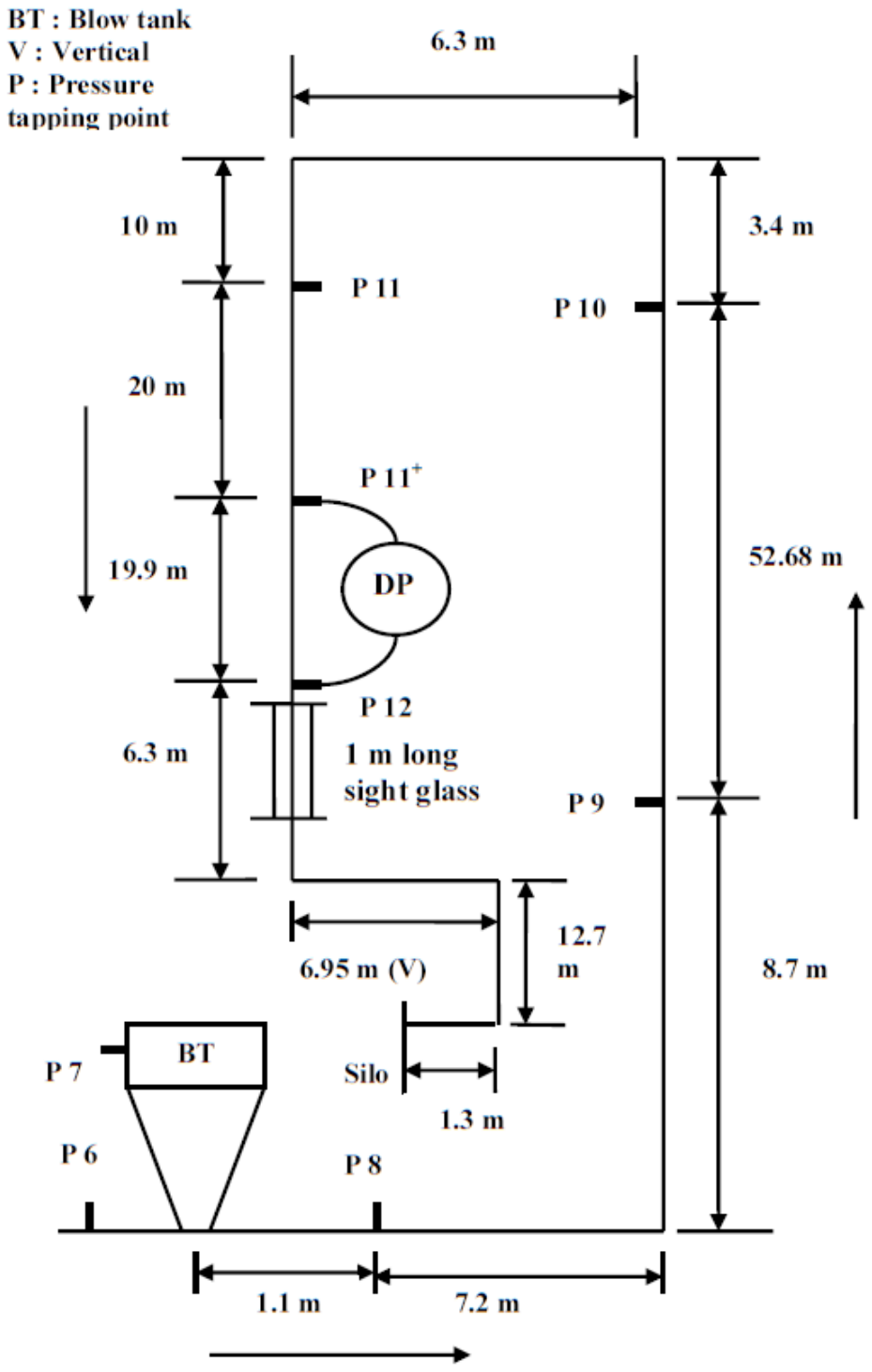

Figure A.1: Layout of the 69 mm I.D. × 148 m long pipeline Test Rig (for White Powder)

Appendix-A2

Table A2 Comparison between experimental and predicted pressure drop (with and without particle size distribution)

S. No.	Inlet air velocity (m/s)	Solid loading ratio	Experiential pressure drop	Predicted pressure drop (without size distribution)	Predicted pressure drop (with size distribution)	% Error of predicting pressure drop (without size distribution)	% Error of predicting pressure drop (with size distribution)
1	12.61	18.77	24418	4233	14518	82.66	40.54
2	9.52	28.18	18579	2972	10597	84.00	42.96
3	9.81	23.91	17765	2875	10117	83.82	43.05
4	12.27	21.94	28646	4430	15726	84.54	45.10
5	11.14	18.40	18999	4069	10363	78.58	45.45
6	12.77	16.76	27691	4212	13814	84.79	50.11
7	11.32	25.13	30415	4327	14965	85.77	50.80
8	11.17	23.40	29592	4047	14121	86.32	52.28
9	7.20	23.74	14182	2134	5857	84.95	58.70